

# Vision language models are *blind*

Pooyan Rahmanzadehgervi<sup>1\*</sup>  
pooyan.rmz@gmail.com

Logan Bolton<sup>1\*</sup>  
logan.bolton@auburn.edu

Mohammad Reza Taesiri<sup>2\*</sup>  
mtaesiri@gmail.com

Anh Totti Nguyen<sup>1</sup>  
anh.ng8@gmail.com

<sup>1</sup> Auburn University, AL, USA

<sup>2</sup> University of Alberta, Canada

**Abstract.** Large language models with vision capabilities (VLMs), *e.g.*, GPT-4o and Gemini-1.5 Pro are powering countless image-text applications and scoring high on many vision-understanding benchmarks. Yet, we find that VLMs fail on 7 visual tasks *absurdly easy* to humans such as identifying (a) whether two circles overlap; (b) whether two lines intersect; (c) which letter is being circled in a word; and (d) counting the number of circles in a Olympic-like logo. The shockingly poor performance of four state-of-the-art VLMs suggests their vision is, at best, like of a person with myopia seeing fine details as blurry, and at worst, like an intelligent person that is blind making educated guesses.

Code is available at: <https://vlmsareblind.github.io/>

**Keywords:** Vision language models · Benchmarks · Geometric primitives

## 1 Introduction

In the last eight months, the advent of VLMs, starting with GPT-4V(ision) [32], has enabled numerous, unprecedented image-text processing applications [42]. VLMs can accurately identify objects in a scene [2, 34, 42] and perform complex tasks based on these detected objects, *e.g.*, calculating the cost of beers on a table from an image of the scene and an image of the menu [43]. Interestingly, VLMs advance so quickly that describing *unusual* activities in an image [37] (*e.g.*, a man ironing on a moving taxi) has become a standard sanity check [13].


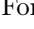
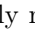
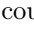

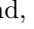

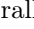

Existing VLM benchmarks [17, 28, 46] cover a wide range of topics but only measure the overall human-vs-LLM gap without pinpointing specific limitations for future vision research. For example, the input images in so many questions, *e.g.*, 42.9% of MMMU [46], are *not* necessary [11]. That is, many answers (1) can be inferred from the textual question and choices alone; and (2) are memorized by VLMs from their Internet-scale training [11]. In sum, while highlighting VLM

---


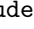
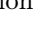
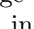
\* All authors contributed to conducting experiments, analyzing results, and writing the paper.

excellence on high-level tests, current benchmarks overlook a key question: **Do VLMs perceive images like humans do?**

In this paper, we test VLMs’ ability to *see* (not reasoning) on low-level vision tasks inspired by the “visual acuity” tests [10] given to humans by optometrists. We test four state-of-the-art (SOTA) VLMs: GPT-4o [4], Gemini-1.5 Pro [35], Claude-3 Sonnet [9], and Claude-3.5 Sonnet [6] on our suite of 8 extremely simple visual tasks that involve only 2D geometric primitives (*e.g.*, lines, circles, and squares) [16] and require minimal to zero world knowledge. Our systematic experiments reveal that the vision of VLMs is surprisingly like that of a person with *myopia*, perceiving fine details as blurry:

1. Despite excellent performance on chart and diagram benchmarks [4,9], VLMs cannot reliably tell whether two lines (or two circles) are intersecting, especially when close together. Accuracy in detecting 0, 1 or 2 intersections in a line chart  of two 2-segment piecewise-linear functions ranges from  $\sim 47\%$  to  $85\%$  (§4.1). For the two-circle  task, VLMs perform better ( $\sim 73\text{--}93\%$  accuracy), but still far from the expected  $100\%$  (§4.2).
2. VLMs can perfectly recognize a circle () and a word (Subdermatoglyphic) separately. Yet, when the circle is superimposed on the word (Subdermatoglyphic), models tend to struggle to identify which letter is being circled (§4.3).
3. VLMs can accurately count shapes, *e.g.*, circles (), that are disjoint and far apart. However, all VLMs struggle to count intersecting circles , (like the Olympic logo), and, generally, primitive shapes (, , ) that are overlapping or nested (§4.4).
4. Tiling up squares into a grid , we find VLMs to shockingly fail to count the number of rows or columns in the grid, whether empty or containing text (§4.5). This is surprising given that VLMs perform so well ( $\geq 90\%$  accuracy) [4,35] on DocVQA [29], which includes many questions with tables.
5. When tasked with tracing colored paths in a simplified subway map of only 2 to 8 paths and a total of 4 stations, VLMs often fail to identify where a path ends, *i.e.*, with an accuracy of  $\sim 23\%$  to  $50\%$  (§4.6).
6. GPT-4o outperforms Gemini-1.5 Pro and Claude-3 Sonnet on 7 prior complex VLM benchmarks [4,35] but performs significantly worse on our tasks (where Gemini-1.5 Pro and Sonnet-3.5 are the best). That is, we reveal surprising VLM limitations that are not measured in prior benchmarks.

## 2 Vision language models

Our goal is to study how SOTA VLMs perceive simple images composed of common geometric primitives interacting. We choose four models: GPT-4o (), Gemini-1.5 Pro (, Gemini-1.5), Claude-3 Sonnet (, Sonnet-3), and Claude-3.5 Sonnet (, Sonnet-3.5) that are ranking highest on 7 recent multimodal vision benchmarks (see [4] and Table 10 in [35]) which cover multi-discipline, college-level subjects in MMMU [46], science diagrams in AI2D [17], mathematics in MathVista [25], charts in ChartQA [28], documents in DocVQA [29], and videos in ActivityNet-QA [45] & EgoSchema [26].

On our benchmark, we find that some chat interfaces perform *worse* than their API counterparts (*e.g.*, the system on `gemini.google.com` is worse than Gemini-1.5 Pro on `aistudio.google.com`) perhaps due to their extra fine-tuning [33] or specific `system` prompts [3] that align VLMs more with a company’s policies. Similarly, we find GPT-4o and Claude 3 models available in `perplexity.ai` to perform worse than the original API models.

**Access** To make sure we test the best VLMs available, we access all four models via their available APIs on `OpenAI`, `Google`, and `Anthropic`.

### 3 BlindTest benchmark of 7 tasks

**Eye exams** Like humans’ visual acuity tests [10], we design a set of 7 very simple, yet novel tasks that are composed of common geometric primitives. We do not use the existing tests designed for human-eye exams for two reasons. First, we avoid using the questions that exist on the Internet, which may provide an inflated measure of vision capabilities [11, 44]. Second, our preliminary experiments show that VLMs *already perform very well* on humans’ eye exams, which typically contain single, separate symbols—*e.g.*, the Snellen chart [10], tumbling E [10], and contrast sensitivity charts [7, 27].

**Motivation** Our `BlindTest` benchmark tests VLMs on identifying known geometric primitives when they are close together, overlapping, or intersecting. We hypothesize that VLMs will struggle because, while the primitives are well-known, their exact spatial information (*e.g.*, the size and position of a  $\bigcirc$ ) on a white canvas is typically not describable in natural language, even for humans, and therefore requires a “visual brain” to perceive. However, VLMs primarily rely on early fusion [23, 38] to integrate a shallow vision encoder into a large language model (LLM), which is essentially a knowledgeable brain without eyes.

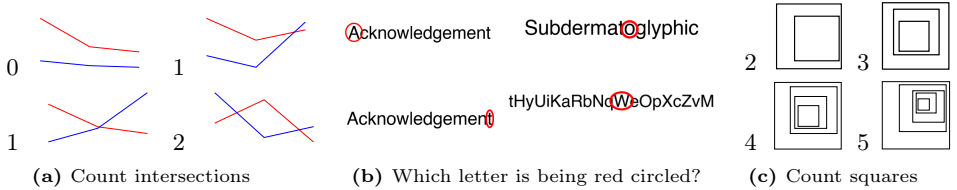
**Controls** For each test image, we prompt VLMs using **two** different, yet semantically equivalent questions. Furthermore, we reproduce the same image using (a) **three** different image sizes and (b) **two** line thickness values when rendering primitives.

#### 3.1 Task 1: Counting line intersections

Given the impressive accuracy of VLMs on answering questions on diagrams and charts (*e.g.*, `Sonnet-3.5` scoring 94.7% on AI2D and 90.8% on ChartQA) [6], a reasonable hypothesis is that VLMs must be able to see whether two graphs intersect in a chart. Here, we test this hypothesis by asking VLMs to count the number of intersections between two 2-segment piece-wise linear functions.

**Images** We create 150 images (Fig. 1a) of 2D line plots drawn on a white canvas. Each line plot consists of two line segments, defined by three points whose

x-coordinates are fixed and equally spaced. The y-coordinates are randomly sampled to create two plots that intersect at exactly 0, 1 or 2 points. See §C.1 for more details.



**Fig. 1:** Images & groundtruth labels from Task 1 (a), Task 3 (b), & Task 5 (c).

**Prompts** We ask each question using two different wordings: (1) “*How many times do the blue and red line plots cross each other?*”; and (2) “*How many times do the blue and red lines intersect?*”

**Groundtruth** answers are  $\in \{0, 1, 2\}$  (random-baseline accuracy: 33%).

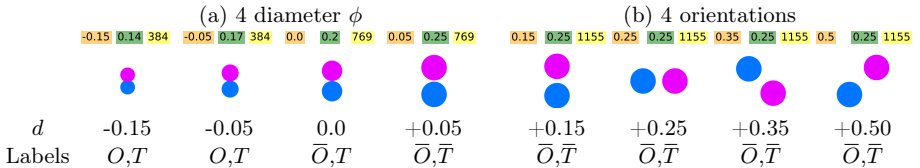
### 3.2 Task 2: Two circles ●●

In the task of counting line intersections (§3.1), each image contains two long, thin colored lines on a large white canvas. Here, we test VLMs in a complementary setting where the two interacting objects (here, two same-sized filled circles ●●) are larger while their gap is smaller. This task evaluates VLM ability in perceiving (1) a small gap between two circles and (2) two circles are overlapping, *i.e.*, no gaps. We vary circle and gap sizes and ask VLMs if two circles are (a) overlapping or (b) touching.

**Images** Given a blank image of size  $C \times C$ , we draw two same-sized circles of diameter  $\phi \in \{\frac{C}{4}, \frac{C}{5}, \frac{C}{6}, \frac{C}{7}\}$  with a boundary-to-boundary distance  $= \phi \times d$  where  $d \in \{-0.15, -0.1, -0.05, 0.0, 0.05, 0.1, 0.15, 0.2, 0.25, 0.3, 0.35, 0.4, 0.45, 0.5\}$  to cover all three cases: overlapping, tangent, and disjoint (see Fig. 2). The two circles are arranged in four different orientations, making a  $90^\circ$ ,  $0^\circ$ ,  $-45^\circ$ , and  $45^\circ$  angle with the x-axis (Fig. 2b). The whole grid sampling generates 224 images per image size. We replicate the procedure for 3 image sizes, *i.e.*,  $C = 384, 769, 1155$  px to create a total of  $3 \times 224 = 672$  images. See §A.1 for more details.


**Prompts** “*Are the two circles touching each other? Answer with Yes/No.*” and “*Are the two circles overlapping? Answer with Yes/No.*”.

**Groundtruth** We consider two circles overlapping and touching ( $O, T$ ) if  $d < 0.0$ ; non-overlapping but touching ( $\bar{O}, T$ ) if  $d = 0.0$ ; and non-overlapping & non-touching ( $\bar{O}, \bar{T}$ ) when  $d > 0.0$  (Fig. 2). Random-baseline accuracy: 50%.

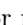


**Fig. 2:** For each image **size** and **distance**  $d$ , we vary **diameter** (a) and orientation (b). Groundtruth:  $O$ : overlapping.  $T$ : touching.  $\bar{O}$ : non-overlapping.  $\bar{T}$ : non-touching.

### 3.3 Task 3: The circled letter Subdermatoglyphic

Consistent with prior reports [36, 42, 43], we find that VLMs can 100% accurately identify a primitive shape (e.g., a red circle ) [36] and can perfectly read an English word (e.g., **Subdermatoglyphic**) alone. Here, we superimposed the red circle on every letter, one at a time, in the word, and ask VLMs to identify which letter is being circled. While the task is easy to humans, our hypothesis is that if a VLM’s vision is “blurry”, it might not be able to identify the exact letter being circled since there is tiny spacing between the adjacent letters.

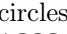

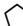
**Images** We choose three strings **Acknowledgement**, **Subdermatoglyphic**, and **tHyUiKaRbNqWeOpXcZvM** because they contain characters of variable widths and heights. Furthermore, all four tested VLMs can read out all characters in these strings when they are input to the models as an image. While **Acknowledgement** is a common English word, **Subdermatoglyphic** is the longest word without repetitive letters. We also test VLMs on the random string **tHyUiKaRbNqWeOpXcZvM** to estimate how much model accuracy is due to its familiarity with the word.

For each (string, circled-letter) pair, we render a  $512 \times 512$  image by choosing among 3 red oval line-thickness levels, 2 font sizes, and 4 random positions in the canvas for a total of 24 images. That is, we generate 360, 408, and 480 images for **Acknowledgement** (15 letters), **Subdermatoglyphic** (17 letters), and **tHyUiKaRbNqWeOpXcZvM** (20 letters), respectively. We ensure each letter to be circled fits completely the oval  (see Fig. 1b). See §B.1 for more details.

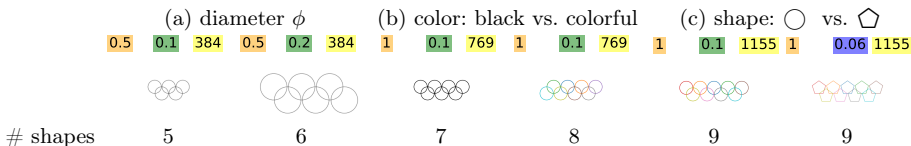
**Prompts** “Which letter is being circled?” and “Which character is being highlighted with a red oval?”.

**Groundtruth** letters need to match predicted letters exactly (case-insensitive).

### 3.4 Task 4: Counting overlapping shapes

Aligned with prior research [43], we also find VLMs to be able to count disjoint circles (). Yet, here, we test VLMs on counting circles that are *intersecting* () like in the Olympic logo—a common cognitive development exercise for preschoolers [1, 5]. Our hypothesis is that a “blurry” vision may not see the intersection between two circles clearly and therefore unable to trace circles and count them. For generalization of our findings, we repeat the experiment with pentagons () as well.

**Images** In an image of size  $C \times C$ , where  $C \in \{384, 769, 1155\}$ px. We draw  $N \in \{5, 6, 7, 8, 9\}$  overlapping, same-sized circles arranged in two rows like the Olympic logo (see Fig. 3). A circle diameter  $\phi \in \{\frac{C}{5}, \frac{C}{10}\}$ . We repeat the images with two different line thickness for rendering circles. This procedure renders 3 resolutions  $\times 5 \times 2$  diameters = 60 images. We repeat for pentagons ( $\diamond$ ) in addition to circles ( $\circ$ ), resulting in  $60 \times 2$  shapes = 120 images in total. For pentagons, their side length  $d \in \{\frac{C}{5}, \frac{C}{10}\}$  See §E.1 for more details.



**Fig. 3:** Images span across three sizes and shapes span across two diameters (and two side lengths for  $\diamond$ ), two color settings, and two line-thicknesses levels.

**Prompts** “How many {shapes} are in the image? Answer with only the number in numerical format.” and “Count the {shapes} in the image. Answer with a number in curly brackets e.g. {3}.” where {shapes} = circles or pentagons.

**Groundtruth** answers are  $\in \{5, 6, 7, 8, 9\}$  (random-baseline accuracy: 20%).

### 3.5 Task 5: Counting the nested squares $\square$


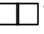

Motivated by the findings that VLMs struggle in counting the intersected circles (§3.4), here, we arrange the shapes differently so that their edges do *not* intersect. That is, each shape is nested entirely inside another (see Fig. 1c). For completeness, we test squares ( $\square$ ) in this task.

**Images** In a canvas of size  $C \times C$ , we render  $N \in \{2, 3, 4, 5\}$  nested squares. The outermost square is rendered first using a random edge length  $d$  and a line thickness  $\in \{2, 3, 4\}$ px. The remaining  $N - 1$  squares are drawn using a size reduction factor,  $0.75 \times d$  and placed at a random coordinate that ensures they do not touch outer squares. For each line thickness, we generate 10 images (where squares have different, random locations) to create  $3 \times 10 = 30$  images. Repeating the process for all  $N$  values results in  $4 \times 30 = 120$  images. See §D.1 for more details.

**Prompts** “Count the total number of squares in the image.”. The results of other counting tasks (§§ 3.1 and 3.4) show that VLM responses remain consistent for alternative tested rephrases, e.g., “How many squares are in the image?”.

**Groundtruth** answers are  $\in \{2, 3, 4, 5\}$  (random-baseline accuracy: 25%).

### 3.6 Task 6: Counting the rows and columns of a grid

The results from prior tasks show VLMs cannot always count shapes that are overlapping (§3.4) or nested  (§3.5). What about adjacent shapes ? Here, we tile up shapes (specifically, ) into a grid and challenge VLMs to count—a task that is supposedly simple to VLMs given their remarkable performance ( $\geq 90\%$  accuracy) [4, 35] on DocVQA [29], which includes many questions with tables. To simplify the task, we ask models to count the number of rows and columns in a given table.

**Images** A grid may have  $N \times N$ ,  $N \times N'$ , or  $N' \times N$  cells, where  $N \in \{3, 4, 5, 6, 7, 8, 9\}$  and  $N' = N + 1$ . Each grid is rendered with two different line-thicknesses on a canvas of size  $C \times C$  where  $C \in \{500, 1250, 2000\}$ px. Besides empty grids, we also replicate the procedure to make grids contain text (which is more common in real-world tables) where each cell contains a single random word (see Fig. 4a). Two versions combined have  $2 \times 222 = 444$  images. See §F.1 for more details.

**Prompts** “Count the number of rows and columns and answer with numbers in curly brackets. For example, *rows={5} columns={6}*” and “How many rows and columns are in the table? Answer with only the numbers in a pair (row, column), e.g., *(5,6)*.”

**Groundtruth** answers include both the number of rows and columns. An answer is correct when both column and row counts are correctly predicted.

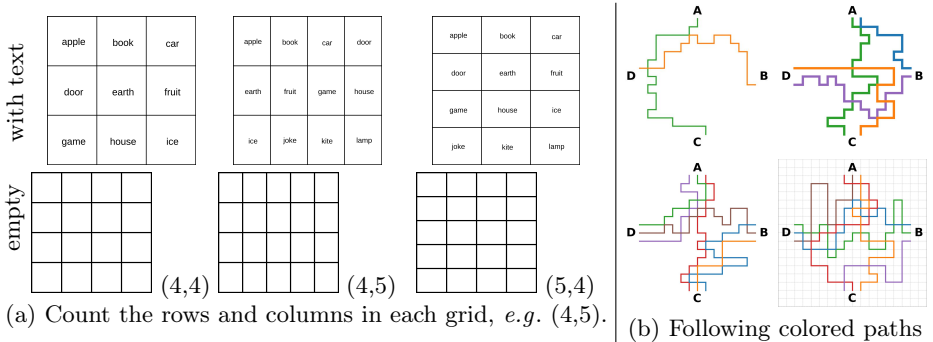
### 3.7 Task 7: Following single-colored paths

It is important for VLMs to be able to follow paths in order to read maps or charts [28], interpret graphs [18], and understand user notations (e.g., arrow) in input images [43]. To assess path-following capability, this task asks models to count the unique-color paths between two given stations in a simplified subway map. This is another easy-to-humans task that challenges VLMs significantly.

**Images** We create each subway map on an image of size  $C \times C$ , where  $C \in \{512, 1024\}$ px (see Fig. 4b). We write 4 station names (A, B, C, D) at 4 fixed coordinates  $\in \{(\frac{C}{2}, C), (C, \frac{C}{2}), (\frac{C}{2}, 0), (0, \frac{C}{2})\}$ , respectively. We divide the canvas into an invisible grid of  $18 \times 18$  cells and initialize 3 path-starting points  $\frac{C}{18}$ px away from each station. We draw a path, using the depth-first search algorithm starting from a random station and a random starting point, where a valid move is one cell in any direction: North, south, east or west. We repeat the process so that each station has exactly  $N \in \{1, 2, 3\}$  outgoing paths, for a total of 180 maps. See §G.1 for details.

**Prompts** “How many single-colored paths go from A to C? Answer with a number in curly brackets, e.g., *{3}*”, and “Count the one-colored routes that go from A to C. Answer with a number in curly brackets, e.g., *{3}*.”

**Groundtruth** answers are  $\in \{0, 1, 2, 3\}$  (random-baseline accuracy: 25%).

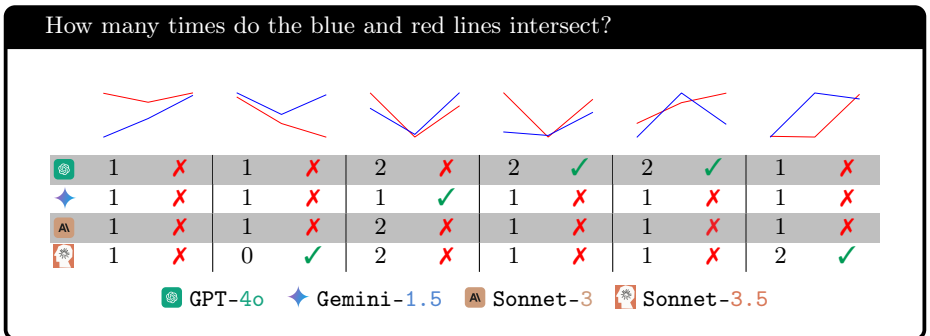


**Fig. 4:** Empty and text-containing grids are generated with various image sizes (a). On an invisible  $18 \times 18$  grid (bottom right), we randomly generate random paths from one station to another (b). Each station has  $N = 1, 2$  or  $3$  outgoing paths per image.

## 4 Results

### 4.1 Task 1: VLMs cannot reliably count line intersections

**Experiment** We parse every model’s free-form response to extract the final answer and then compare it to the groundtruth. When there is no intersection, models usually respond with “*there are no intersections*”, which we label “0”. We report the mean accuracy of every model on two prompts and analyze the sensitivity of the accuracy to varying spatial parameters.







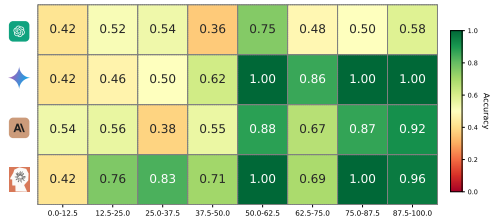
**Fig. 5:** VLMs cannot reliably count the intersections between the blue and red plots.

**Results** First, across two prompts and three line widths, all VLMs perform poorly on this easy task (Fig. 5). The best accuracy is only 77.33% (Sonnet-3.5) (Table 1). More specifically, **VLMs tend to perform worse when the distance between two plots narrows** (Fig. 6). As each line plot is composed of three key points, the distance between two plots is computed as the mean



**Table 1:** The accuracy breakdown by line width, averaged over two prompts, shows that VLMs cannot reliably count the intersections between two simple 2D line plots.

Line width				
2 px	45.00	70.00	64.00	80.00
3 px	47.00	68.00	66.00	79.00
4 px	54.00	71.00	62.00	73.00
Mean	48.67	69.67	64.00	<b>77.33</b>



**Fig. 6:** The x-axis shows the mean, normalized distance over 3 pairs of points of two 2-segment plots. VLMs tend to be confused when two plots are close together.



distance over three corresponding point pairs. See §C.4 for more samples of VLM predictions. VLMs perform similarly across three line widths (§C.2) and two prompts (§C.3).

Our findings are in stark contrast to the high accuracy of VLMs on ChartQA [4, 35], suggesting that VLMs can recognize the overall trend of a line plot but unable to “zoom in” to see fine details, *e.g.*, which lines are intersecting.

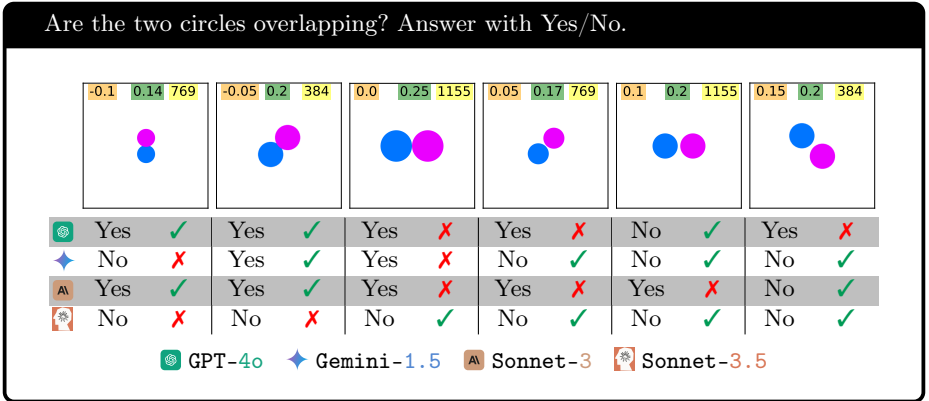
## 4.2 VLMs cannot clearly see if two circles overlap or not

Motivated by VLM poor performance in counting line intersections (§4.1), here, we replace lines by large, filled circles and ask VLMs explicitly if the two circles are touching (or overlapping) or not.

**Experiment** Since we instruct VLMs to output a binary answer (Yes/No), we use Python to extract VLMs’ formatted answer from their responses for comparing with groundtruth.

**Results** Surprisingly, even on this task where objects ( ) are large and clearly visible to humans, no VLMs are able to solve it perfectly (Fig. 7). The best accuracy is 92.78% (Gemini-1.5) over all images and prompts (Table 2). A common trend is **when two circles are close together, VLMs tend to perform poorly**, making educated guesses, *e.g.*, Sonnet-3.5 often answer “No” conservatively (Fig. 7). Shockingly, GPT-4o (the worst accuracy) is not 100% accurate even when the distance between two circles is as large as one radius (Fig. 8;  $d = 0.5$ ). That is, VLM vision seems not clear enough to see the fine gap or intersection between two circles.

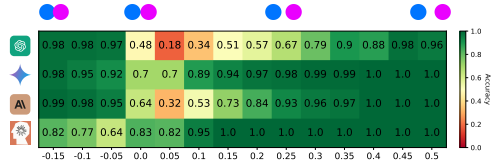
VLMs often perform consistently across three image resolutions (§A.2); however, interestingly, every model performs consistently the best at a specific circle orientation (§A.5). More examples of VLMs’ answers are in §A.7.



**Fig. 7:** VLMs consistently fail at smaller **distances**. However, when the **gap** is large and clearly visible, GPT-4o remains unreliable (rightmost). **Sonnet-3.5** tends to conservatively answer “No” regardless of the actual distance between the two circles.

**Table 2:** GPT-4o and Gemini-1.5 perform more consistently over the two different prompts (“overlapping” and “touching”) than Sonnet-3 and Sonnet-3.5.

Model	Overlapping	Touching	Mean
<span style="color: green;">●</span>	71.27	74.10	72.69
<span style="color: blue;">◆</span>	<b>93.30</b>	92.26	<b>92.78</b>
<span style="color: orange;">■</span>	88.09	80.95	84.52
<span style="color: red;">■</span>	88.83	<b>94.49</b>	91.66



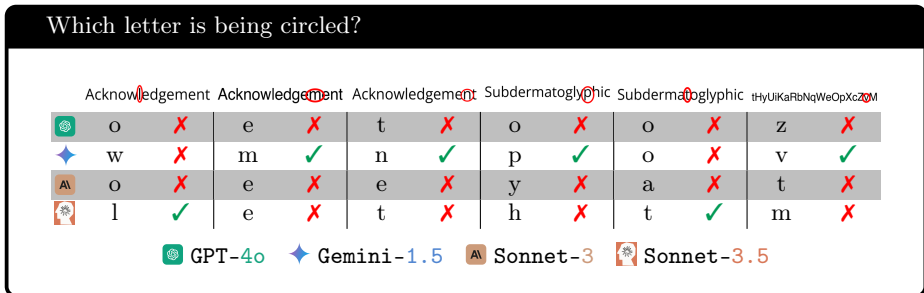
**Fig. 8:** VLMs perform poorly when two circles are tangent ( $d = 0.0$ ) or close together ( $d = 0.05, 0.10$ ). Yet, **Sonnet-3.5** is better at  $d \geq 0.0$ . (perhaps due to its tendency to answer “No”).

### 4.3 VLMs do not always see the letter inside the red circle

**Experiment** We use simple text processing and regex matching to extract the answer since each model’s output follows a specific format, *e.g.*, GPT-4o’s responses typically contain a single line explaining its answer, with the predicted letter mostly placed between quotation marks ('). However, Gemini-1.5 uses markdown formatting and places double asterisks (\*\*) around the letter.

**Results** First of all, we find that all VLMs can accurately spell out the string despite there is a red oval ○ superimposed. Yet, interestingly, reading out which letter is being circled turns out to pose a challenge to all VLMs (Fig. 9). For example, VLMs tend to make mistakes when the letter is slightly, partially occluded by the red oval (*e.g.*, Subd<sup>er</sup>matoglyphic).

**When making mistakes, VLMs often predict letters adjacent to the one being circled** (see the confusion matrix in Fig. 10 and more results in §B.2).



**Fig. 9:** Identifying the letter being circled is non-trivial for VLMs across both English words (Acknowledgement & Subdermatoglyphic) and a random string (tHyUiKaRbNqWeOpXcZvM). When making mistakes, VLMs tend to predict letters adjacent to the circled one.

**Table 3:** Except for GPT-4o (🌀), all models perform better on the two English words than on the random string, suggesting that VLMs might leverage their familiarity with characters in a known word to make educated guesses.

String	🌀	🔹	🏠	🏠
Acknowledgement	69.03	97.50	82.64	91.11
Subdermatoglyphic	63.60	91.05	71.45	94.49
tHyUiKaRbNqWeOpXcZvM	77.92	89.90	65.94	82.08
Mean accuracy	70.18	92.81	73.34	89.22

Sometimes models hallucinate, *e.g.*, coming up with characters non-existent in Subdermatoglyphic (*e.g.*, “9”, “n”, “©”) despite that it can accurately spell out the word (see Fig. 10). More failure cases are reported in §§ B.3 and B.6.

Except for GPT-4o, all models perform slightly better (by 2 to 6 points) on the two English words compared to the random string (Table 3), suggesting that **knowing the word might help VLMs make better educated guesses, slightly improving accuracy**. Gemini-1.5 and Sonnet-3.5 are the top-2 models (92.81% and 89.22%) and better than GPT-4o and Sonnet-3 by a large margin of nearly +20 points (Table 3). VLMs perform similarly across two prompts (§B.5) and two font types (§B.4).

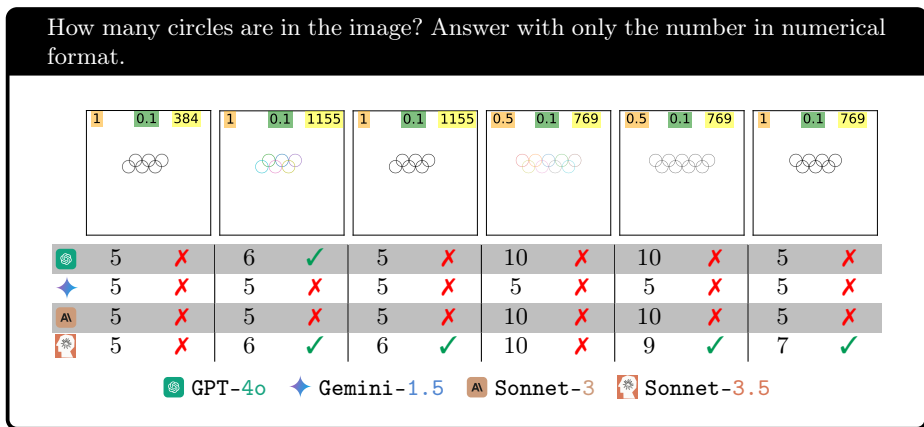
Circled Letter	s	186	2	0	0	0	0	0	0	0	0	0	0	0	0	0	0	0	2	0	0	2	0	0	0	0	
	u	5	167	14	0	0	0	0	0	0	0	0	0	6	0	0	0	0	0	0	0	0	0	0	0	0	
	b	0	12	168	7	0	0	0	0	0	0	0	0	5	0	0	0	0	0	0	0	0	0	0	0	0	
	d	0	0	9	167	2	0	0	0	0	0	0	14	0	0	0	0	0	0	0	0	0	0	0	0	0	
	e	0	0	0	4	171	0	0	0	0	0	0	17	0	0	0	0	0	0	0	0	0	0	0	0	0	
	r	0	0	0	2	11	134	0	1	0	0	0	43	0	0	0	0	0	0	0	0	0	0	0	1	0	
	m	0	0	0	2	2	19	161	2	0	0	0	4	0	0	0	0	0	0	0	0	0	0	1	1	0	
	a	0	0	0	0	0	0	0	183	0	3	0	0	0	0	0	0	0	0	0	0	6	0	0	0	0	
	t	0	0	0	0	0	0	0	34	101	55	0	1	0	0	0	1	0	0	0	0	0	0	0	0	0	
	o	0	0	0	0	0	0	0	0	0	192	0	0	0	0	0	0	0	0	0	0	0	0	0	0	0	
	g	0	0	0	0	0	0	0	0	0	23	167	0	0	0	0	0	0	0	2	0	0	0	0	0	0	
	l	0	0	0	0	0	0	0	0	0	49	14	108	21	0	0	0	0	0	0	0	0	0	0	0	0	
	y	0	0	0	0	0	0	1	0	0	29	5	18	137	2	0	0	0	0	0	0	0	0	0	0	0	
	p	0	0	0	0	0	0	0	0	0	67	1	0	19	99	6	0	0	0	0	0	0	0	0	0	0	
	h	0	0	3	0	0	0	1	0	0	2	0	0	0	10	167	9	0	0	0	0	0	0	0	0	0	
	i	0	0	0	0	0	0	1	0	0	7	0	0	0	0	6	167	11	0	0	0	0	0	0	0	0	
	c	0	0	0	0	0	0	0	0	0	26	0	0	0	0	0	16	141	0	0	0	0	0	0	0	9	
		š	ú	û	đ	ë	ř	ǎ	ť	o	g	i	ý	p	h	i	c	9	@	None	ma	n	©				
		Predicted Letter																									

**Fig. 10:** Aggregate confusion matrix summed over all four VLMs and 48 images per model for the word **Subdermatoglyphic**. Each row sums  $48 \text{ images} \times 4 \text{ models} = 192$ . All models accurately predict the letter “o” in the middle. Models mostly mispredict to characters near the circled letter. Interestingly, VLMs sometimes hallucinate characters that do not even exist in **Subdermatoglyphic**, e.g., “9” or “n” (right panel).

#### 4.4 VLMs struggle to count overlapped and nested shapes

**Experiment** We run all VLMs on all images of overlapping circles and pentagons (§3.4) and nested squares (§3.5). We prompt models to output the count in a formatted answer. We extract templated answers and compare them without groundtruth. For each shape (circles, pentagons and squares), we run two different prompts.

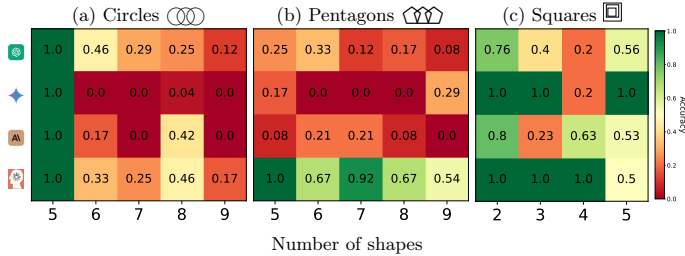
**Results** Regardless of whether the shapes are overlapped or nested (*i.e.*, their edges intersect or not) both cases appear to be challenging to VLMs (Fig. 11). On nested squares, model accuracies vary widely—GPT-4o (48.33%) and Sonnet-3 (55.00%) are at least 30 points behind Gemini-1.5 (80.00%) and Sonnet-3.5 (87.50%). This gap is even larger on counting overlapped circles and pentagons—Sonnet-3.5 is better than the rest by multiple times (*e.g.*, 75.83% vs. 9.16% of Gemini-1.5; Table 4).



**Fig. 11:** Counting overlapped circles is not easy to VLMs regardless of circle colors, line widths, and resolutions. Gemini-1.5 often predicts “5” regardless of the actual circle count, suggesting a strong bias towards the well-known Olympic logo.

**Table 4:** Counting nested squares (a) is easier than counting overlapping circles (b) and pentagons (c) for VLMs. Sonnet-3.5 performs better than the rest by a large margin on all three shapes.

Shape	🌐	🔹	AI	🌐
(a) Squares	48.33	80.00	55.00	<b>87.50</b>
(b) Circles	42.50	20.83	31.66	<b>44.16</b>
(c) Pentagons	19.16	9.16	11.66	<b>75.83</b>



**Fig. 12:** All four VLMs can count 5 overlapping circles (x-axis), but only **Sonnet-3.5** can count 5 overlapping pentagons (b). Counting from 6–9 shapes (either  $\bigcirc$  or  $\bigcirc$ ) is challenging to VLMs. Interestingly, **GPT-4o** (🟢) and **Sonnet-3** (🟡) are unable to reliably count even two nested squares (c).

All four models are 100% accurate in counting 5 circles. Yet, surprisingly adding only a single circle is sufficient to cause accuracy to dip substantially near zero (Fig. 12; column 6–9). However, in counting pentagons, all VLMs (except **Sonnet-3.5**) perform poorly even at 5 pentagons. Overall, **counting from 6 to 9 shapes (both circles and pentagons) is hard to all models.**

This contrast suggests that VLMs are biased towards the well-known Olympic logo, which has 5 circles. When there are more than five circles ( $\bigcirc$ ) and VLMs predict an incorrect count, **Gemini-1.5** predicts “5” 98.95% of the time regardless of the actual number of circles (Table 5). For other models, this frequency is also much higher than that in the case of pentagons. Our results show strong evidence that **VLMs are biased towards the well-known 5-circle Olympic logo.** More details on this bias are in §E.4.

**GPT-4o** performs better on colored shapes than on black shapes and **Sonnet-3.5** is increasingly better as the image size increases. However, the accuracy of **all other models only change marginally as we change colors (§E.3) and resolutions (§E.2).**

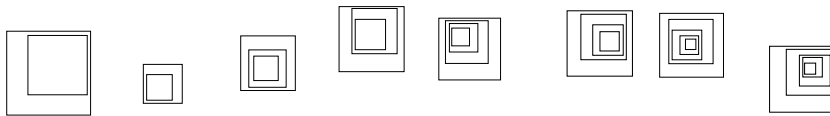
**Table 5:** Frequency (%) of predicting “5” when there are more than 5 circles ( $\bigcirc$ ) or pentagons ( $\bigcirc$ ), *i.e.*,  $N = 6, 7, 8, 9$  shapes in the image. **Gemini-1.5** 98.95% of the time predicts “5” circles but this tendency disappears in the case of  $\bigcirc$  (1.04%), showing the strongest bias towards the 5-circle Olympic logo (among four models).





🟢		🔵		🟠		🟡	
$\bigcirc$	$\bigcirc$	$\bigcirc$	$\bigcirc$	$\bigcirc$	$\bigcirc$	$\bigcirc$	$\bigcirc$
14.58	2.08	98.95	1.04	59.37	23.95	43.75	15.62





Note that there are only 2 to 5 squares in each image in the task of counting nested squares and these squares do not intersect (Fig. 13). Surprisingly, **GPT-4o** and **Sonnet-3** still struggle to count two or three nested squares (Fig. 12c).

When the count increases to four and five, all models are far from 100% accurate. Our results show that it is not easy for VLMs to extract accurate representation of shapes even when their edges do not intersect.

Count total number of squares in the image.



	1	✗	2	✓	1	✗	6	✗	10	✗	5	✗	1	✗	5	✓
	2	✓	2	✓	3	✓	3	✓	5	✗	5	✗	5	✓	5	✓
	2	✓	3	✗	4	✗	4	✗	5	✗	4	✓	5	✓	9	✗
	2	✓	2	✓	3	✓	3	✓	4	✓	4	✓	5	✓	1	✗

 GPT-4o  
 Gemini-1.5  
 Sonnet-3  
 Sonnet-3.5

**Fig. 13:** Counting nested squares is not easy to VLMs even when there are only two squares (leftmost). The task becomes harder as the count increases from 2 to 5. **Sonnet-3.5** performs the best (87.50%) but still not at the 100% by humans.

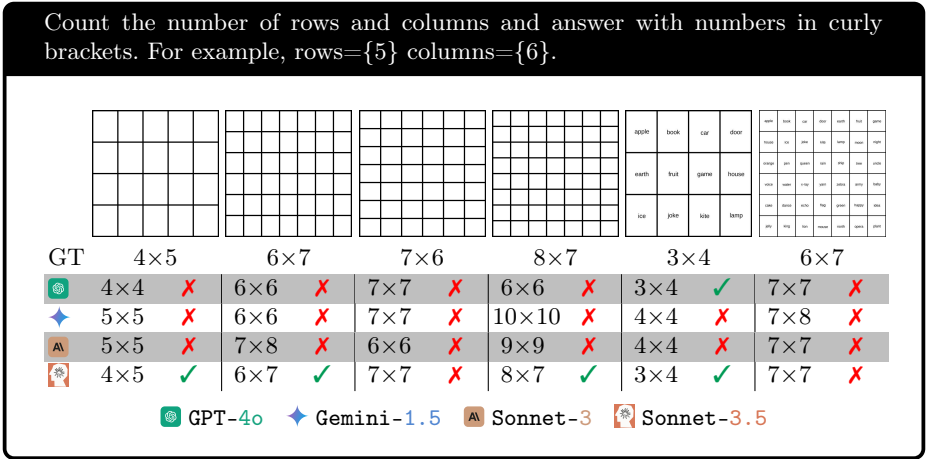
#### 4.5 VLMs cannot easily count the rows and columns in a grid

Since VLMs struggle in counting the number of simple shapes when the shape edges intersect (§3.4) or separate (§3.5), here, we test the remaining case where these shapes are placed adjacently sharing edges, specifically, tiling up multiple rectangles into a single grid. Given the impressive accuracy of VLMs [4, 6, 35] on questions involving tables and spreadsheets in DocVQA [29], we hypothesize that VLMs must be able to count the rows and columns in a grid.

**Experiment** We run all VLMs on the images of empty grids and text-containing grids (§3.6) and analyze their formatted answers.

**Results** First, VLMs surprisingly often struggle to count the exact number of rows and columns in an empty grid (see Table 6). Specifically, they are often off by 1 or 2 (e.g., GPT-4o predicts 4×4 and Gemini-1.5 predicts 5×5 for a 4×5 grid; Fig. 14). This finding suggests that VLMs can extract important content from a table to answer table-related questions in DocVQA [29] but cannot clearly see a table cell-by-cell.

This might be because tables in documents are mostly non-empty and VLMs are not used to them. Interestingly, after attempting to make the task easier by **adding a single word to each cell, we observe the accuracy of all VLMs to increase substantially** (e.g., 26.13% to 53.03% for GPT-4o) (Table 6). Yet,



**Fig. 14:** VLMs are often off by one or two in counting rows and columns in an empty grid. The same is true when a grid is small (*e.g.*, 3×4) and contains a word in each cell.

**Table 6:** Including text inside grids improves all model accuracies. **Sonnet-3.5**, yet, outperforms other models on both empty and text-containing grids.

Grid type	🟢	🔵	🟡	🔴
Empty	26.13	25.75	25.00	59.84
Text	<b>53.03</b>	<b>45.83</b>	<b>47.34</b>	<b>88.68</b>
Mean	39.58	35.79	36.17	74.26

**Table 7:** Except **Sonnet-3.5** and **Gemini-1.5**, VLMs do not see single-colored paths even when only one path exists each station.

Paths	🟢	🔵	🟡	🔴
1	67.50	85.41	23.75	<b>95.00</b>
2	44.37	28.75	37.18	<b>56.25</b>
3	<b>36.71</b>	25.78	15.42	25.39
Mean	45.89	40.01	23.78	<b>50.18</b>

no models can solve this task with the best model (**Sonnet-3.5**) performing at 88.68% on text-containing grids and 59.84% on empty grids (Fig. 15a vs. b).

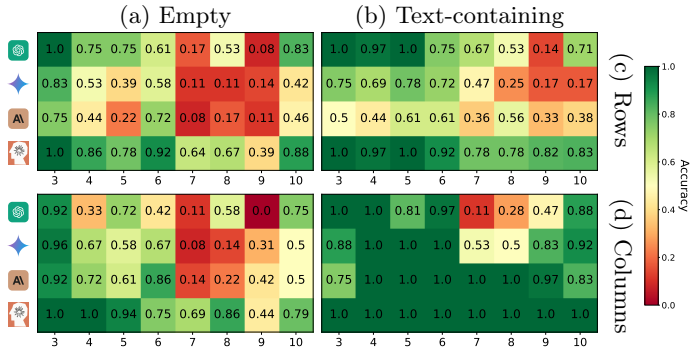
We also find most models (**Gemini-1.5**, **Sonnet-3**, and **Sonnet-3.5**) to perform consistently better in counting columns than counting rows (Fig. 15c vs. d). See §F.2 and §F.3 for more results.

#### 4.6 VLMs struggle to trace and to count single-colored paths

This task test a VLM’s ability in recognizing a path of a unique color and *trace* it from a given starting station to the destination, an important task in reading maps and graphs in general [28].

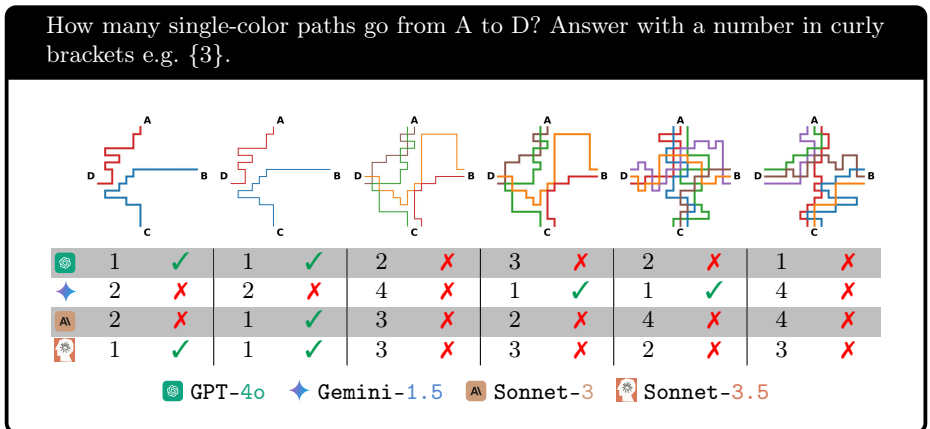
**Experiment** From a subway map (§3.7), we randomly pick 2 stations and prompt every model to count the single-colored paths between them. We then extract answers from the templated answers and compare them with the groundtruth.





**Fig. 15:** Accuracy of counting rows (c) vs. columns (d) (here, analyzed separately) when the grids are empty (a) vs. contain text (b). VLMs (especially, 🔹 and AI) generally count much more accurately when grids contain text (b) vs. empty grids (a). Interestingly, columns (d) are also easier for VLMs to count than rows (d).

**Results** Shockingly, we find that even when there is only *one path* between two stations, no models can reach 100% accuracy (the best is **Sonnet-3.5** at 95%; Table 7 and the worse is 23.75%). VLM predictions are often off by 1 to 3 paths (Fig. 16). Most of VLMs perform worse as the complexity of the maps increases from 1 to 3 paths. More samples of VLM responses are in §G.2.



**Fig. 16:** Some VLMs (🔹, AI) surprisingly fail in even extremely easy cases (leftmost). As the number of paths exiting each station increases, VLMs tend to perform worse.

## 5 Related Work

**Benchmarking VLM vision understanding** College-level topics [46], charts [28], documents [29] or videos [45] are among the common benchmarks for assessing VLM vision understanding [4, 6, 9, 35] and are witnessing VLMs’ recent rapid progress—*e.g.*, **Sonnet-3.5** is reaching 95.2% on DocVQA, 90.8% on ChartQA, and 94.7% on AI2D [6]. However, most of vision benchmarks attempt to evaluate VLMs on real-world, topic-specific data that require extensive prior knowledge [11, 19, 41], which has a “data leakage” problem, *i.e.*, VLMs many times can answer accurately without even the input image [11]. Furthermore, most benchmarks test VLMs on the data that humans have to deal with to provide a high-level sense of the human-machine intelligence gap [24, 44]. In contrast, our **BlindTest** benchmark differs significantly from prior benchmarks because it is (1) **extremely easy to humans and can be solved by a 5-year-old** (unlike [28, 29, 46]); (2) the first low-level, visual sanity check for VLMs; (3) requiring minimal to zero prior knowledge; (4) requiring zero commonsense or complex reasoning (unlike [12, 47])—*i.e.*, **a strong language model is of little use here when it is non-natural for humans to describe BlindTest images in language** (for a brain thinking in language step-by-step to solve it).

The ARC benchmark [12, 31] also contain abstract images made up of simple shapes; however they challenge VLMs on understanding and reasoning based on those patterns. ARC assumes VLMs can identify the abstract shapes in order to reason. In contrast, our **BlindTest** directly evaluates VLM capabilities in recognizing the primitive shapes.

**Improving VLM vision capabilities** Most recent recipes for improving SOTA VLMs involve finetuning a pretrained LLM coupled with vision encoders to solve high-level vision tasks [22]. Such late-fusion approaches fuse visual representations learned from the tokenized image with a powerful thinking brain [20, 21, 30].

However, current vision approaches for VLMs are facing challenges as models sometimes are “blind”—unable to see natural objects exist in a real photo [40]. In contrast, we are showing VLMs are visually impaired at low-level abstract images, *e.g.*, inability to count 6 overlapping circles or 3 nested squares. Our circled letter §3.3 is inspired by VLM abilities in recognizing content inside a red circle over real objects in natural images [36, 42, 43]. However, we show that VLMs can fail at a low-level, optical character recognition as opposed to recognizing real objects. To the best of our knowledge, no prior attempts have been made to address the exact limitations raised in our paper: (1) identifying and counting simple lines, shapes and geometric primitives when they interact (§4.1 to §4.5); (2) following colored paths (§4.6). Solving these limitations may be the foundation for VLMs to progress on some existing vision benchmarks on graphs, *e.g.*, [18], visual math [25] and blindness in natural images (*e.g.*, understanding the direction an object is facing [40]).

## 6 Discussion and Conclusion

We propose **BlindTest**, a benchmark of seven novel low-level visual tasks that did not exist on the Internet before and requires minimal to zero knowledge. By design, our tasks minimize the chance that VLMs can solve by memorization or by not using the input image—an issue in some prior benchmarks [11].

We document shocking findings that the best commercial VLMs are still struggling with tasks that can be easily solved by a five-year-old (*e.g.*, telling whether two circles or lines intersect §4.2). These limitations may be largely due to the late-fusion approach [8, 23] of integrating vision into an LLM model and that early-fusion [38, 39] may be the way forward. We find that simply finetuning a 7B, SOTA late-fusion open-source VLM [14] using LORA on our tasks does not yield a high-performing model (§A.6). That is, training a single model that performs well on **BlindTest** might be non-trivial, interesting research direction.

### Acknowledgement

We thank Hung H. Nguyen, Thang Pham, Ali Yildirim, Giang Nguyen, and Tin Nguyen at Auburn University for feedback and discussions of the earlier results. We are also thankful for the API research credits from Anthropic to MRT. AN was supported by the NSF Grant No. 1850117 & 2145767, and donations from NaphCare Foundation & Adobe Research.

## References

1. Count shapes printables | myteachingstation.com. <https://www.myteachingstation.com/preschool/math/numbers/count-shapes-printables>, (Accessed on 07/05/2024)
2. Gemini spatial example. <https://gemini-spatial-example.grantcuster.com/>, (Accessed on 05/31/2024)
3. Gpt-4 system prompt revealed - by patrick mcguinness. <https://patmcguinness.substack.com/p/gpt-4-system-prompt-revealed>, (Accessed on 06/06/2024)
4. Hello gpt-4o | openai. <https://openai.com/index/hello-gpt-4o/>, (Accessed on 05/31/2024)
5. How many counting game with color simple geometric shapes for kids, educational maths task for the development of logical thinking, preschool worksheet activity, count and write the result, vector stock vector by ©olya.by@mail.ru 266096226. <https://depositphotos.com/vector/how-many-counting-game-with-color-simple-geometric-shapes-for-kids-educational-maths-task-for-266096226.html>, (Accessed on 07/05/2024)
6. Introducing claude 3.5 sonnet \ anthropic. <https://www.anthropic.com/news/claude-3-5-sonnet>, (Accessed on 07/03/2024)
7. Vision screening. <https://www.zeiss.com/vision-care/us/eye-health-and-care/vision-screening.html>, (Accessed on 07/03/2024)
8. Alayrac, J.B., Donahue, J., Luc, P., Miech, A., Barr, I., Hasson, Y., Lenc, K., Mensch, A., Millican, K., Reynolds, M., et al.: Flamingo: a visual language model for few-shot learning. *Advances in neural information processing systems* **35**, 23716–23736 (2022)
9. Anthropic, A.: The claude 3 model family: Opus, sonnet, haiku. *Claude-3 Model Card* (2024)
10. Bailey, I.L., Lovie-Kitchin, J.E.: Visual acuity testing. from the laboratory to the clinic. *Vision research* **90**, 2–9 (2013)
11. Chen, L., Li, J., Dong, X., Zhang, P., Zang, Y., Chen, Z., Duan, H., Wang, J., Qiao, Y., Lin, D., et al.: Are we on the right way for evaluating large vision-language models? *arXiv preprint arXiv:2403.20330* (2024)
12. Chollet, F.: On the measure of intelligence. *arXiv preprint arXiv:1911.01547* (2019)
13. Dai, W., Li, J., Li, D., Tiong, A.M.H., Zhao, J., Wang, W., Li, B., Fung, P., Hoi, S.: Instructblip: Towards general-purpose vision-language models with instruction tuning (2023)
14. He, M., Liu, Y., Wu, B., Yuan, J., Wang, Y., Huang, T., Zhao, B.: Efficient multimodal learning from data-centric perspective. *arXiv preprint arXiv:2402.11530* (2024)
15. He, M., Liu, Y., Wu, B., Yuan, J., Wang, Y., Huang, T., Zhao, B.: Efficient multimodal learning from data-centric perspective. *arXiv preprint arXiv:2402.11530* (2024)
16. Hughes, J.F.: *Computer graphics: principles and practice*. Pearson Education (2014)
17. Kembhavi, A., Salvato, M., Kolve, E., Seo, M., Hajishirzi, H., Farhadi, A.: A diagram is worth a dozen images. In: *Computer Vision—ECCV 2016: 14th European Conference, Amsterdam, The Netherlands, October 11–14, 2016, Proceedings, Part IV* 14. pp. 235–251. Springer (2016)

18. yunxin li, Hu, B., Shi, H., Wang, W., Wang, L., Zhang, M.: Visiongraph: Leveraging large multimodal models for graph theory problems in visual context. In: Forty-first International Conference on Machine Learning (2024), <https://openreview.net/forum?id=gjoUXwuZdy>
19. Liang, Z., Guo, K., Liu, G., Guo, T., Zhou, Y., Yang, T., Jiao, J., Pi, R., Zhang, J., Zhang, X.: Scemqa: A scientific college entrance level multimodal question answering benchmark. arXiv preprint arXiv:2402.05138 (2024)
20. Liu, H., Li, C., Li, Y., Lee, Y.J.: Improved baselines with visual instruction tuning (2023)
21. Liu, H., Li, C., Li, Y., Li, B., Zhang, Y., Shen, S., Lee, Y.J.: Llava-next: Improved reasoning, ocr, and world knowledge (January 2024), <https://llava-vl.github.io/blog/2024-01-30-llava-next/>
22. Liu, H., Li, C., Wu, Q., Lee, Y.J.: Visual instruction tuning. arXiv preprint arXiv:2304.08485 (2023)
23. Liu, H., Li, C., Wu, Q., Lee, Y.J.: Visual instruction tuning. Advances in neural information processing systems **36** (2024)
24. Liu, Y., Duan, H., Zhang, Y., Li, B., Zhang, S., Zhao, W., Yuan, Y., Wang, J., He, C., Liu, Z., et al.: Mmbench: Is your multi-modal model an all-around player? arXiv preprint arXiv:2307.06281 (2023)
25. Lu, P., Bansal, H., Xia, T., Liu, J., Li, C., Hajishirzi, H., Cheng, H., Chang, K.W., Galley, M., Gao, J.: Mathvista: Evaluating mathematical reasoning of foundation models in visual contexts. In: International Conference on Learning Representations (ICLR) (2024)
26. Mangalam, K., Akshulakov, R., Malik, J.: Egoschema: A diagnostic benchmark for very long-form video language understanding. Advances in Neural Information Processing Systems **36** (2024)
27. Mäntyjärvi, M., Laitinen, T.: Normal values for the pelli-robson contrast sensitivity test. Journal of Cataract & Refractive Surgery **27**(2), 261–266 (2001)
28. Masry, A., Do, X.L., Tan, J.Q., Joty, S., Hoque, E.: ChartQA: A benchmark for question answering about charts with visual and logical reasoning. In: Muresan, S., Nakov, P., Villavicencio, A. (eds.) Findings of the Association for Computational Linguistics: ACL 2022. pp. 2263–2279. Association for Computational Linguistics, Dublin, Ireland (May 2022). <https://doi.org/10.18653/v1/2022.findings-acl.177>, <https://aclanthology.org/2022.findings-acl.177>
29. Mathew, M., Karatzas, D., Jawahar, C.: Docvqa: A dataset for vqa on document images. In: Proceedings of the IEEE/CVF winter conference on applications of computer vision. pp. 2200–2209 (2021)
30. McKinzie, B., Gan, Z., Fauconnier, J.P., Dodge, S., Zhang, B., Dufter, P., Shah, D., Du, X., Peng, F., Weers, F., Belyi, A., Zhang, H., Singh, K., Kang, D., Jain, A., He, H., Schwarzer, M., Gunter, T., Kong, X., Zhang, A., Wang, J., Wang, C., Du, N., Lei, T., Wiseman, S., Yin, G., Lee, M., Wang, Z., Pang, R., Gräsch, P., Toshev, A., Yang, Y.: Mml: Methods, analysis & insights from multimodal llm pre-training. ArXiv [abs/2403.09611](https://arxiv.org/abs/2403.09611) (2024), <https://api.semanticscholar.org/CorpusID:268384865>
31. Mitchell, M., Palmairini, A.B., Moskvichev, A.K.: Comparing humans, GPT-4, and GPT-4v on abstraction and reasoning tasks. In: AAAI 2024 Workshop on "Are Large Language Models Simply Causal Parrots?" (2023), <https://openreview.net/forum?id=3rGT50kzpc>
32. OpenAI: Gpt-4 technical report (2023)

33. Ouyang, L., Wu, J., Jiang, X., Almeida, D., Wainwright, C., Mishkin, P., Zhang, C., Agarwal, S., Slama, K., Ray, A., et al.: Training language models to follow instructions with human feedback. *Advances in neural information processing systems* **35**, 27730–27744 (2022)
34. Rasheed, H., Maaz, M., Shaji, S., Shaker, A., Khan, S., Cholakkal, H., Anwer, R.M., Xing, E., Yang, M.H., Khan, F.S.: Glamm: Pixel grounding large multimodal model. *The IEEE/CVF Conference on Computer Vision and Pattern Recognition* (2024)
35. Reid, M., Savinov, N., Teplyashin, D., Lepikhin, D., Lillicrap, T., Alayrac, J.b., Soricut, R., Lazaridou, A., Firat, O., Schrittwieser, J., et al.: Gemini 1.5: Unlocking multimodal understanding across millions of tokens of context. *arXiv preprint arXiv:2403.05530* (2024)
36. Shtedritski, A., Rupprecht, C., Vedaldi, A.: What does clip know about a red circle? visual prompt engineering for vlms. In: *2023 IEEE/CVF International Conference on Computer Vision (ICCV)*. pp. 11953–11963. IEEE Computer Society, Los Alamitos, CA, USA (oct 2023). <https://doi.org/10.1109/ICCV51070.2023.011101>, <https://doi.ieeecomputersociety.org/10.1109/ICCV51070.2023.011101>
37. Taesiri, M.R., Feng, T., Bezemer, C.P., Nguyen, A.: Glitchbench: Can large multimodal models detect video game glitches? In: *Proceedings of the IEEE/CVF Conference on Computer Vision and Pattern Recognition*. pp. 22444–22455 (2024)
38. Team, C.: Chameleon: Mixed-modal early-fusion foundation models. *arXiv preprint arXiv:2405.09818* (2024)
39. Tong, S., Brown, E., Wu, P., Woo, S., Middepogu, M., Akula, S.C., Yang, J., Yang, S., Iyer, A., Pan, X., et al.: Cambrian-1: A fully open, vision-centric exploration of multimodal llms. *arXiv preprint arXiv:2406.16860* (2024)
40. Tong, S., Liu, Z., Zhai, Y., Ma, Y., LeCun, Y., Xie, S.: Eyes wide shut? exploring the visual shortcomings of multimodal llms. In: *Proceedings of the IEEE/CVF Conference on Computer Vision and Pattern Recognition (CVPR)*. pp. 9568–9578 (June 2024)
41. Wang, K., Pan, J., Shi, W., Lu, Z., Zhan, M., Li, H.: Measuring multimodal mathematical reasoning with math-vision dataset (2024)
42. Yang, J., Zhang, H., Li, F., Zou, X., Li, C., Gao, J.: Set-of-mark prompting unleashes extraordinary visual grounding in gpt-4v (2023), <https://arxiv.org/abs/2310.11441>
43. Yang, Z., Li, L., Lin, K., Wang, J., Lin, C., Liu, Z., Wang, L.: The dawn of llms: Preliminary explorations with gpt-4v(ision). *CoRR* **abs/2309.17421** (2023). <https://doi.org/10.48550/ARXIV.2309.17421>, <https://doi.org/10.48550/arXiv.2309.17421>
44. Yu, W., Yang, Z., Li, L., Wang, J., Lin, K., Liu, Z., Wang, X., Wang, L.: Mm-vet: Evaluating large multimodal models for integrated capabilities. In: *International conference on machine learning*. PMLR (2024)
45. Yu, Z., Xu, D., Yu, J., Yu, T., Zhao, Z., Zhuang, Y., Tao, D.: Activitynet-qa: A dataset for understanding complex web videos via question answering. In: *Proceedings of the AAAI Conference on Artificial Intelligence*. vol. 33, pp. 9127–9134 (2019)
46. Yue, X., Ni, Y., Zhang, K., Zheng, T., Liu, R., Zhang, G., Stevens, S., Jiang, D., Ren, W., Sun, Y., Wei, C., Yu, B., Yuan, R., Sun, R., Yin, M., Zheng, B., Yang, Z., Liu, Y., Huang, W., Sun, H., Su, Y., Chen, W.: Mmmu: A massive multi-discipline multimodal understanding and reasoning benchmark for expert agi. In: *Proceedings of CVPR* (2024)

47. Zellers, R., Bisk, Y., Farhadi, A., Choi, Y.: From recognition to cognition: Visual commonsense reasoning. In: Proceedings of the IEEE/CVF conference on computer vision and pattern recognition. pp. 6720–6731 (2019)

## A Two touching circles task

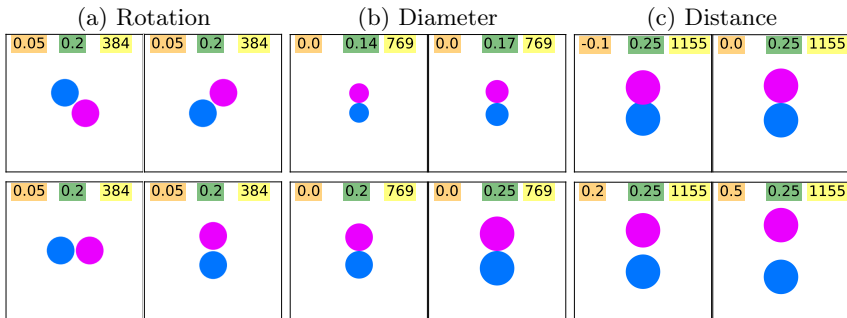
### A.1 Benchmark Construction Details

To create our benchmark, we use 5 parameters to control the diversity of the samples.

- **Color:** We fix the colors for each circle to use  $\{magenta, dodgerblue\}$ .
- **Image size:** We use the physical size, and the DPI arguments in *matplotlib* to initialize the image size. The physical size is fixed to  $5 \times 5$ , and the DPI  $\in \{100, 200, 300\}$ . The output image sizes are  $\{384, 769, 1155\}$ px.
- **Diameter:** We use uniform diameters for both circles and choose the value proportional to the image size, where the diameter is  $\{\frac{1}{4}, \frac{1}{5}, \frac{1}{6}, \frac{1}{7}\}$  of the image size.
- **Distance:** The boundary-to-boundary distance between circles is a fraction of the diameter chosen from  $\{-0.15, -0.1, -0.05, 0.0, 0.05, 0.1, 0.15, 0.2, 0.25, 0.3, 0.35, 0.4, 0.45, 0.5\}$ . Based on our definition, center-to-center distance is  $(2+distance) \times diameter$ .
- **Rotation:** We include 2 main rotations (vertical and horizontal), and 2 diagonal rotations.

We use the center of the image as the origin so that it always aligns with the midpoint of distances between two circles. This systematic process results in a benchmark comprising 672 images (see Fig. 17).

**Code** The code is available at <https://anonymous.4open.science/r/Benchmark-85F0/src/TouchingCircle/TwoTouchingCircles.ipynb>.



**Fig. 17:** Samples in the benchmark include various settings for drawing two circles. We start with choosing a rotation (a) and change other parameters of each plot, *e.g.*, **the diameter** (b), **the distance** between perimeters (c), and the **image size** (in pixels). We show the parameters that can be changed to generate different samples inside the legend.



## A.2 Finding: image resolution does not affect VLMs performance

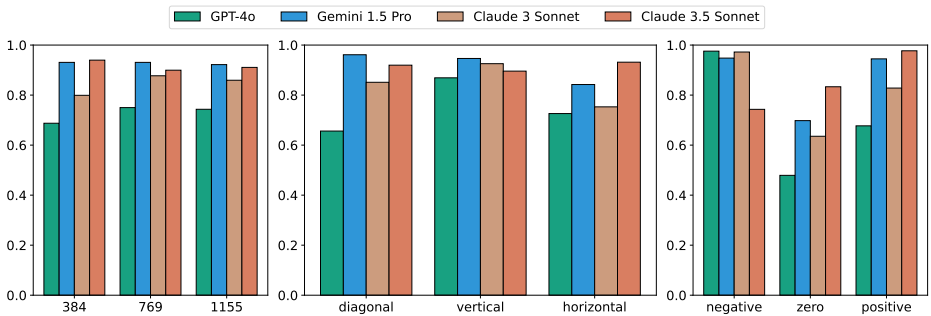
Fig. 18-left shows that VLMs are almost invariant to the image resolution. For instance, GPT-4o and Sonnet-3’s performance saturates at 769px, and Sonnet-3.5 slightly performs worse at 769 and 1155px compared to 384px. Gemini-1.5, however, is more consistent across different resolutions. That is, seeing the intersection of two circles does not depend on the quality of the image.

## A.3 Finding: the vertical rotation closes the gap between models’ performance

As shown in Fig. 18-middle, arranging the circles in vertical rotation causes the models to perform similarly on the benchmark. Although Gemini-1.5 slightly performs better at diagonal and Sonnet-3.5 at horizontal rotation, VLMs perform relatively better at vertical rotation. This suggests that the task complexity due to various rotations is not the main source of low performance in VLMs.

## A.4 Finding: Increasing the distance improves the VLMs’ accuracy

VLMs perform better when the distance increases from zero to positive values (see Fig. 18-right). However, Sonnet-3.5 is more conservative than other VLMs that mostly answer “Yes”, which results in its lowest performance at negative distances.







**Fig. 18:** There is no correlation between the resolution of the image (left) and VLMs’ performance. Across various rotations (middle), VLMs perform almost the same at vertical. Most failure cases are at boundary distances (right).

## A.5 Finding: VLMs prefer a specific rotation

Table 8 shows that VLMs prefer different rotations. For example, GPT-4o performs best at vertical, Gemini-1.5 at diagonal, Sonnet-3.5 at horizontal, and Sonnet-3 at vertical.

**Table 8:** VLM accuracy is often best at a specific two-circle orientation. Across three different resolutions, GPT-4o and Sonnet-3 perform much better when two circles are arranged vertically. In contrast, Gemini-1.5 and Sonnet-3.5 prefer the diagonal and horizontal orientations, respectively.

Resolution	Rotation					
<i>a</i>	384px	VERTICAL	<b>78.57</b>	93.75	<b>95.53</b>	91.07
	HORIZONTAL	67.85	88.39	72.32	<b>96.42</b>	
	DIAGONAL	64.28	<b>95.08</b>	75.88	94.19	
<i>b</i>	769px	VERTICAL	<b>91.07</b>	94.64	<b>91.96</b>	89.28
	HORIZONTAL	77.67	83.92	81.25	<b>90.17</b>	
	DIAGONAL	67.40	<b>96.87</b>	88.83	90.17	
<i>c</i>	1155px	VERTICAL	<b>89.28</b>	95.53	90.17	88.39
	HORIZONTAL	72.32	80.35	72.32	<b>92.85</b>	
	DIAGONAL	67.85	<b>96.42</b>	<b>90.62</b>	91.51	

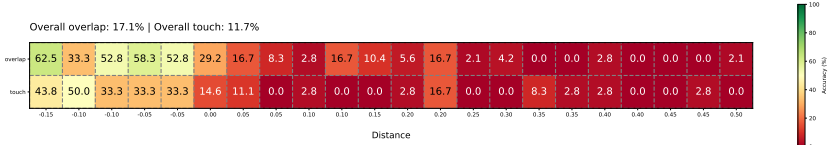
## A.6 Results for fine-tuning Bunny on the two touching circle

In order to determine if fine-tuning could improve the model’s performance on this task we attempted to fine-tune Bunny [15] on the two touching circles task. We fine-tuned Bunny using datasets of sizes: 10K, 20K, 50K, and 100K samples, each containing a balanced number of instances where the circles are either overlapping or separate (equal number of YES/NO answers in the training set).

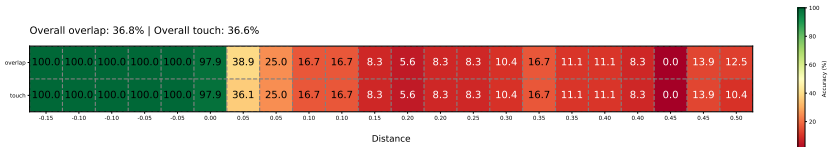
The baseline model, without any fine-tuning, achieved 17.1% accuracy for task overlap and 11.7% for touching circles. After fine-tuning, we observed improvements with smaller datasets, such as 10K and 20K cases, where accuracy reached up to 36.8%. However, increasing the number of samples did not lead to better performance. In some instances, such as with the 50K dataset, the model failed to predict anything and only generated the *end-of-text* token.

The loss values for all these experiments were very close to zero, indicating that the model overfits the training set but fails to generalize. This suggests that training on this task is not straightforward and may require a combination of multiple tasks or that this problem does not have a simple solution.

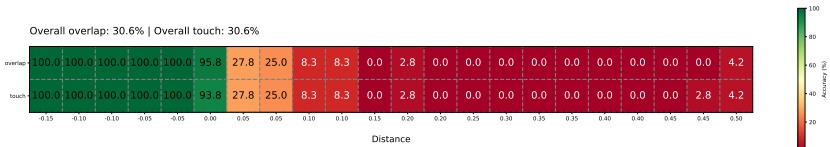
Fig. 19 shows the accuracy breakdown by distance of the two circles. The model’s performance improves when the circles are overlapping, but when there is a long distance between them, the model does not generalize well and cannot provide accurate answers.



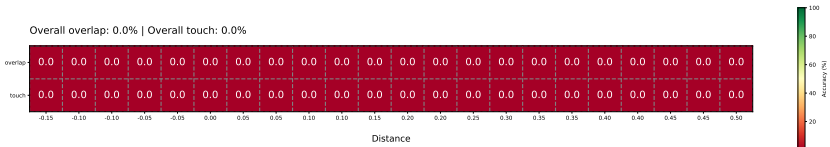
(a) Accuracy by distance without fine-tuning



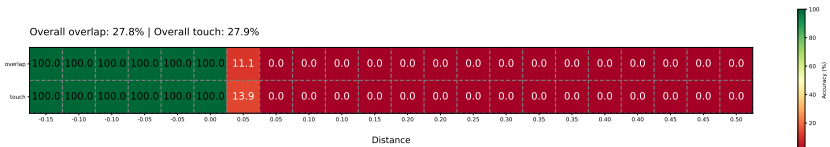
(b) Accuracy by distance with 10K samples



(c) Accuracy by distance with 20K samples



(d) Accuracy by distance with 50K samples

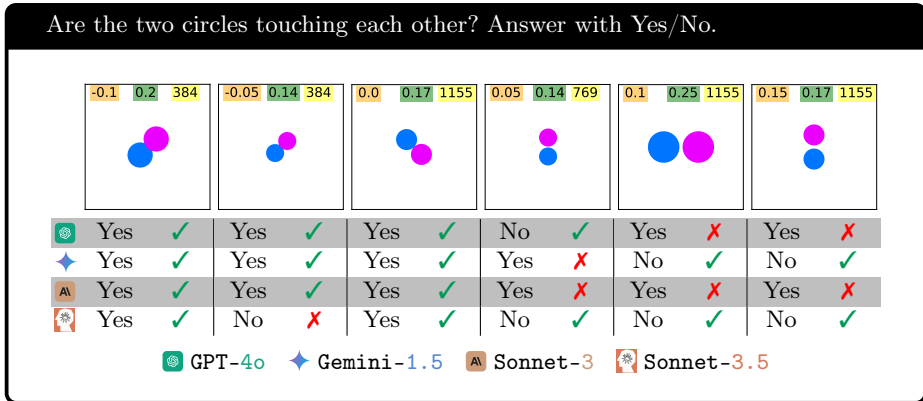


(e) Accuracy by distance with 100K samples

Fig. 19: Comparison of Bunny’s accuracy by distance with and without fine-tuning

## A.7 Additional examples

We show examples of models' responses to the prompts on the two touching circles task in Fig. 20.



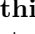



**Fig. 20:** Some VLMs consistently fail by not seeing the distance between the two circles at large **distances** and **resolutions** (GPT-4o and Sonnet-3-rightmost). Gemini-1.5 and Sonnet-3 also cannot see the small gaps ( $distance=0.0$ )

## B Task 3: Identifying circled letter in word

### B.1 Task construction

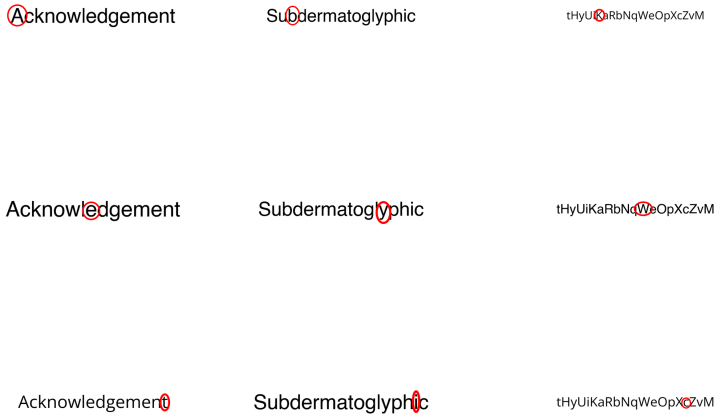
Each image is created using a combination of the below variables.

- **Word:** The word is chosen among 3 candidates {**Acknowledgement**, **Subdermatoglyphic**, **tHyUiKaRbNqWeOpXcZvM** }. Each word has unique features, *e.g.*, variable letter size (**Acknowledgement**), non-repetitive letters (**Subdermatoglyphic**), and non-existing word (**tHyUiKaRbNqWeOpXcZvM**).
- **Letter:** We draw the oval () over all the letters in a word.
- **Font:** We use 2 different font styles for each word, **OpenSans** and **Helvetica**.
- **Oval () thickness:** We generate the  with 3 various line thicknesses.
- **Scaling factor:** Since each letter has a unique size, we use a scaling factor to control the size of the .
- **Padding:** We use four values for padding {25, 50, 100, 200}, by which we change the word’s position on the image. This ensures that the word is not always in the center of the image.

Finally, we render the text on a white canvas with a size of  $512 \times 512$  pixels, and we get 180 images for **Acknowledgement**, 204 for **Subdermatoglyphic**, and 240 samples for **tHyUiKaRbNqWeOpXcZvM** (see Fig. 21).

**Code** The code is available at <https://anonymous.4open.science/r/Benchmark-85F0/src/CircledWord/GenerateSamples.ipynb>.

**Post-processing:** We do not ask VLMs to provide answers in a pre-defined format. Instead, we write code to extract predicted labels from VLM free-form response.



(a) Acknowledgement (b) Subdermatoglyphic (c) tHyUiKaRbNqWeOpXcZvM

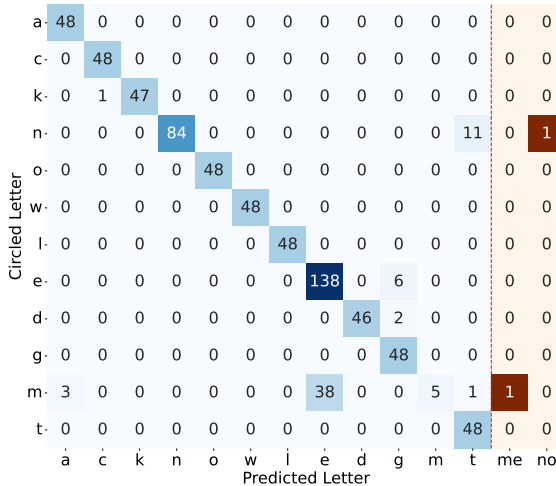
**Fig. 21:** Our benchmark comprises three different words, of which one letter is circled by the red oval in each image.

## B.2 Finding: VLMs mostly confuse the adjacent character for the circled letter

Models often mistake the neighboring characters as the circled letter (see Table 9), GPT-4o 33.67% in the word *Subdermatoglyphic* (the lowest) and Sonnet-3.5 90.62% in the word *Acknowledgement* (the highest). Fig. 22 depicts that in the word *Acknowledgement*, where letter “m” is surrounded by two “e”, Sonnet-3.5 mispredicts “e” for “m” 38 times out of 48 (79.16%). Gemini-1.5, in the word *tHyUiKaRbNqWeOpXcZvM*, where letters “K” and “a” are adjacent, mispredicts “a” for “K” 35 times out of 48 (72.91%) (see Fig. 23).

**Table 9:** Frequency (%) of predicting the adjacent letters when the model makes wrong predictions. VLMs cannot accurately see the position of the red oval in the image, which causes them to mispredict the adjacent letters.

Word	Adjacent Character
🕶️ Acknowledgement	63.68
🕶️ Subdermatoglyphic	33.67
🕶️ tHyUiKaRbNqWeOpXcZvM	66.98
🔹 Acknowledgement	44.44
🔹 Subdermatoglyphic	78.08
🔹 tHyUiKaRbNqWeOpXcZvM	77.32
🟡 Acknowledgement	60.00
🟡 Subdermatoglyphic	58.37
🟡 tHyUiKaRbNqWeOpXcZvM	55.66
🏠 Acknowledgement	90.62
🏠 Subdermatoglyphic	84.44
🏠 tHyUiKaRbNqWeOpXcZvM	50.00



**Fig. 22:** Adjacent letters are the most common wrong prediction for **Sonnet-3.5** in **Acknowledgement**, e.g., letter “e” is predicted instead of “m” 79.16% of the time, or letter “t” is predicted instead of “n” 22.91% of the time.

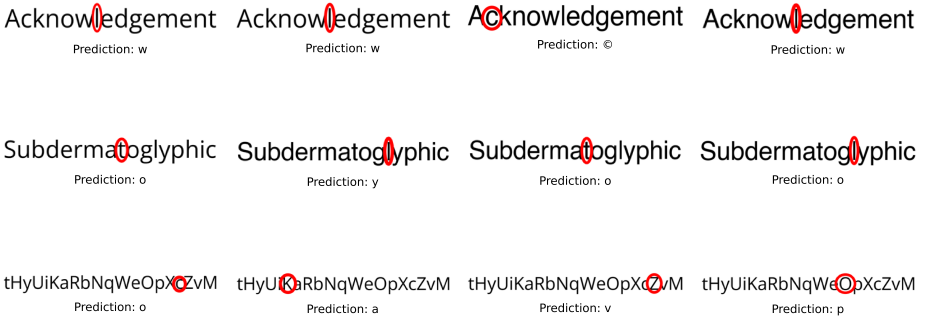
t	48	0	0	0	0	0	0	0	0	0	0	0	0	0	0	0	0	0	0	0	0	0	0
h	0	46	2	0	0	0	0	0	0	0	0	0	0	0	0	0	0	0	0	0	0	0	0
y	0	0	48	0	0	0	0	0	0	0	0	0	0	0	0	0	0	0	0	0	0	0	0
u	0	0	0	47	1	0	0	0	0	0	0	0	0	0	0	0	0	0	0	0	0	0	0
i	0	0	0	0	48	0	0	0	0	0	0	0	0	0	0	0	0	0	0	0	0	0	0
k	0	0	0	0	0	13	35	0	0	0	0	0	0	0	0	0	0	0	0	0	0	0	0
a	0	0	0	0	0	0	43	0	0	0	0	0	0	0	0	0	0	0	0	0	0	0	5
r	0	0	0	0	0	0	0	42	6	0	0	0	0	0	0	0	0	0	0	0	0	0	0
b	0	0	0	0	0	0	0	0	48	0	0	0	0	0	0	0	0	0	0	0	0	0	0
n	0	0	0	0	0	0	0	0	0	48	0	0	0	0	0	0	0	0	0	0	0	0	0
q	0	0	0	0	0	0	0	0	0	0	45	0	0	0	0	0	0	0	0	0	0	0	3
w	0	0	0	0	0	0	0	0	0	0	0	48	0	0	0	0	0	0	0	0	0	0	0
e	0	0	0	0	0	0	0	0	0	0	0	0	48	0	0	0	0	0	0	0	0	0	0
o	0	0	0	0	0	0	0	0	0	0	0	0	0	46	2	0	0	0	0	0	0	0	0
p	0	0	0	0	0	0	0	0	0	0	0	0	0	0	48	0	0	0	0	0	0	0	0
x	0	0	0	0	0	0	0	0	0	0	0	0	0	0	0	34	14	0	0	0	0	0	0
c	0	0	0	0	0	0	0	0	0	0	0	0	0	14	0	0	34	0	0	0	0	0	0
z	0	0	0	0	0	0	0	0	0	0	0	0	0	0	0	0	0	33	15	0	0	0	0
v	0	0	0	0	0	0	0	0	0	0	0	0	0	0	0	0	0	0	48	0	0	0	0
m	0	0	0	0	0	0	0	0	0	0	0	0	0	0	0	0	0	0	0	0	48	0	0
t	h	y	u	i	k	á	r	b	n	q	w	e	o	p	x	c	z	v	m	@	g		

**Fig. 23:** Gemini-1.5’s accuracy breaks on 3 scenarios in the word tHyUiKaRbN-qWeOpXcZvM, 1) predicting the adjacent letters (“a” instead of “K”), 2) confusing the red oval as a part of the circled letter (“@” instead of “a”), and 3) similarity in the shape of the letters (“g” instead of “q” or “o” instead of “c”).



### B.3 Finding: GPT-4o and Gemini-1.5 confuse the red oval as part of the letter

Figs. 24 and 25 show that Gemini-1.5 and GPT-4o sometimes fail to recognize that the red oval is not part of the letter. Gemini-1.5 predicts “o” when the circled letter is not “o” (see Fig. 24), and GPT-4o often predicts “o” regardless of what letter is circled (Fig. 25). Gemini-1.5 also predicts “©” instead of “c”, and GPT-4o predicts “@” instead of “a”.



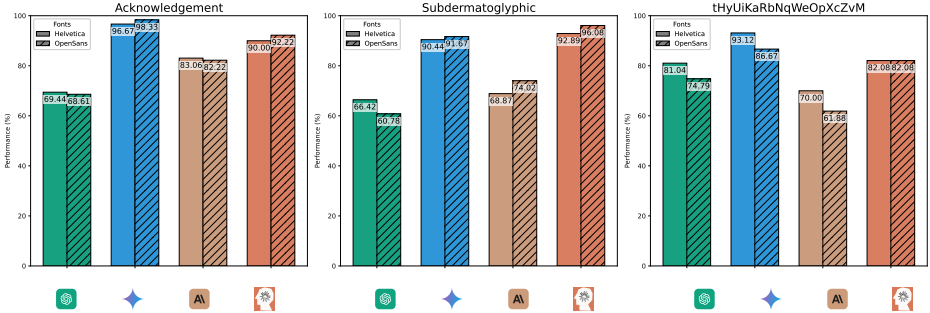
**Fig. 24:** Random samples for different words, and Gemini-1.5’s predictions, where Gemini-1.5 mostly predicts the adjacent letters or confuses the red oval as part of the circled letter.

s	48	0	0	0	0	0	0	0	0	0	0	0	0	0	0	0	0	0
u	5	40	2	0	0	0	0	0	0	1	0	0	0	0	0	0	0	0
b	0	10	30	4	0	0	0	0	0	4	0	0	0	0	0	0	0	0
d	0	0	6	32	2	0	0	0	0	8	0	0	0	0	0	0	0	0
e	0	0	0	1	47	0	0	0	0	0	0	0	0	0	0	0	0	0
r	0	0	0	1	3	5	0	1	0	38	0	0	0	0	0	0	0	0
m	0	0	0	1	2	3	36	2	0	4	0	0	0	0	0	0	0	0
a	0	0	0	0	0	0	0	39	0	3	0	0	0	0	0	0	0	6
t	0	0	0	0	0	0	0	0	28	20	0	0	0	0	0	0	0	0
o	0	0	0	0	0	0	0	0	0	48	0	0	0	0	0	0	0	0
g	0	0	0	0	0	0	0	0	0	13	35	0	0	0	0	0	0	0
l	0	0	0	0	0	0	0	0	0	42	4	0	2	0	0	0	0	0
y	0	0	0	0	0	0	0	0	0	26	3	2	17	0	0	0	0	0
p	0	0	0	0	0	0	0	0	0	38	0	0	1	8	1	0	0	0
h	0	0	0	0	0	0	0	0	0	2	0	0	0	10	33	3	0	0
i	0	0	0	0	0	0	0	0	0	5	0	0	0	0	0	37	6	0
c	0	0	0	0	0	0	0	0	0	12	0	0	0	0	0	0	36	0
	s	u	b	d	e	r	m	a	t	o	g	l	y	p	h	i	c	@

**Fig. 25:** GPT-4o is the most sensitive to confuse the red oval as part of the letter, where it often predicts “o” instead of “l”, “y”, “p”, and “c” in the word **Subdermatoglyphic**.

## B.4 Finding: font selection does not vary the performance of the models

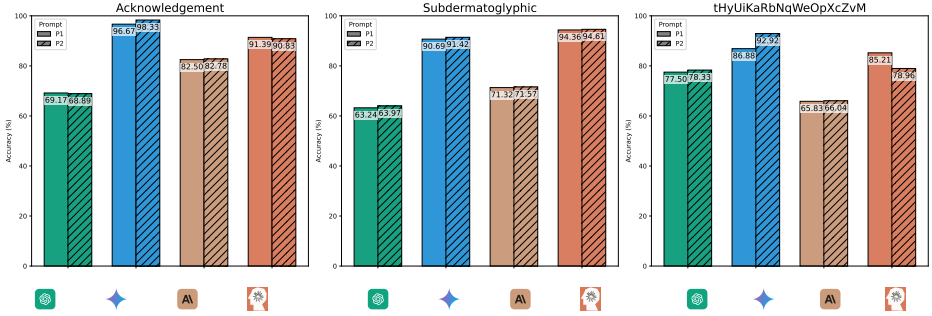
As shown in Fig. 26, models do not show a significant variance over different fonts, suggesting our choice of font is not a reason for their ill-performance.



**Fig. 26:** VLMs do not show significant variance over different fonts. This suggests that using different spacing between letters, letter styles, and letter size has minimal effects on the VLMs’ ability to see the content of the red oval.

## B.5 Finding: models are invariant to our choice of prompts

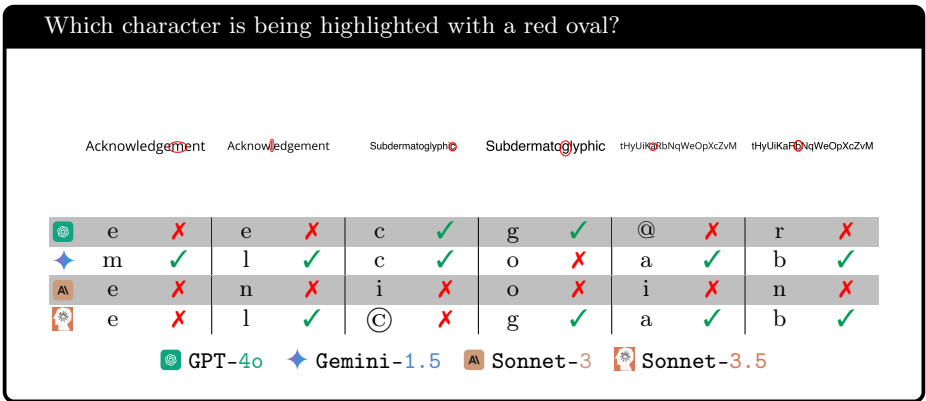
Our choice of prompts has almost no impact on the performance of the models as depicted in Fig. 27.



**Fig. 27:** Model performance breakdown for different prompts P1: *Which letter is being circled?* and P2: *Which character is being highlighted with a red oval?* highlights that regardless of the prompts, VLMs perform similarly in seeing the contents of the red oval.

## B.6 Additional Examples

Examples from our evaluation of VLMs on the circled letter task are shown in Fig. 28



**Fig. 28:** Most failure cases consist of predicting the adjacent letters (predicting “e” instead of “m” in GPT-4o, Sonnet-3, and Sonnet-3.5 leftmost), and confusing the red oval as part of the circled letter (predicting “©” instead of “c” in Sonnet-3.5).

## C Counting the number of line intersections task

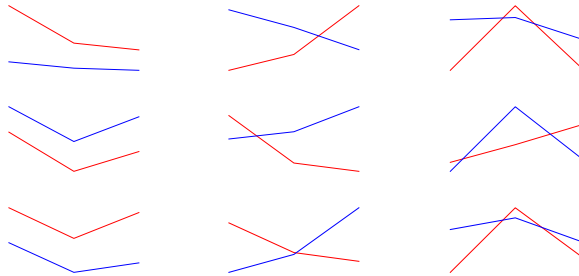
### C.1 Benchmark Construction Details

To create our benchmark, we use 5 parameters to control the diversity of the samples.

- **Color:** We fix the colors for each line to use  $\{blue, red\}$
- **X-coordinate:** For each line, we choose three uniformly distributed x coordinates on the canvas to plot the x values of lines.
- **Y-coordinate:** We randomly pick three y values for each line on the canvas.
- **Line thickness:** We vary the line thicknesses with standard *matplotlib* values (2, 3, and 4).
- **Number of intersections:** We count the intersections based on the three points defined for each line  $((x, y_1), (x, y_2), \text{ and } (x, y_3))$ .

We repeat the process until we have 50 samples of 0, 1, and 2 intersections, resulting in 150 images (see Fig. 29).

**Code** The code is available at <https://anonymous.4open.science/r/Benchmark-85F0/src/LineIntersection/GenerateSamples.ipynb>.

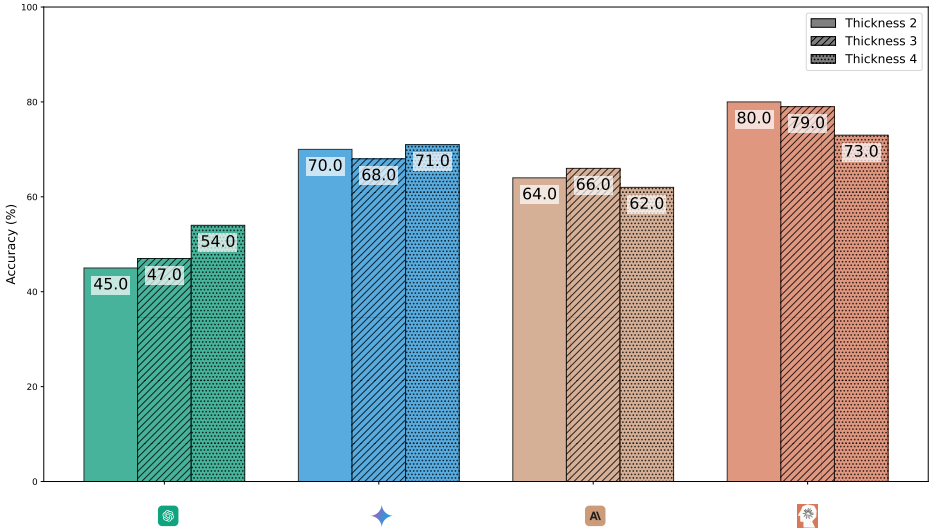


(a) zero intersection (b) one intersection (c) two intersections

**Fig. 29:** Samples from the two intersecting lines benchmark that contain 0, 1, or 2 line intersections.

## C.2 Finding: line thickness does not influence VLM ability to count line intersections

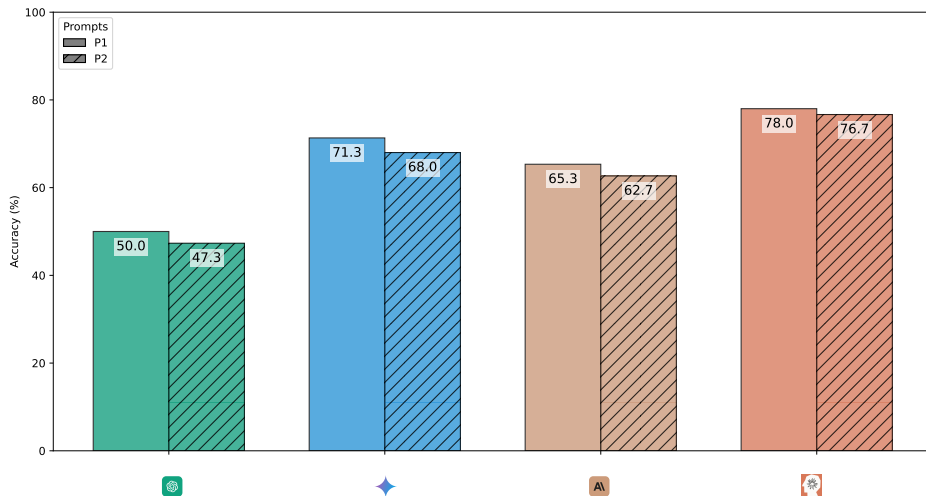
Fig. 30 depicts that increasing the line thickness in our plots does not help the VLMs see and count the intersections of 2D lines. Interestingly, **Sonnet-3.5** performs best on the thinnest line which suggests the model can see the thin lines, but intersections are not clear to its vision.



**Fig. 30:** Gemini-1.5 and Sonnet-3.5 having their best performance on the thinnest line suggests that VLMs can already see the lines, yet cannot reliably see and count the intersections.

### C.3 Finding: different prompts result in similar accuracy

Our choice of prompts has minimal impact on the models' performance as shown in Fig. 31.

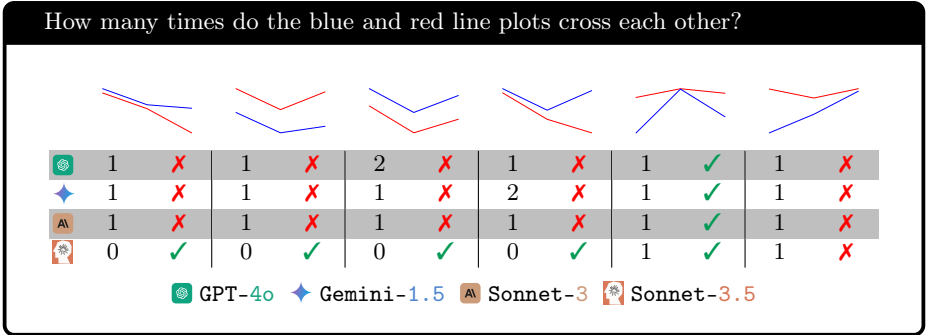


**Fig. 31:** Performance breakdown by different prompts, P1: *How many times do the blue and red line plots cross each other?* and P2: *How many times do the blue and red lines intersect?* shows that models slightly perform differently, yet do not show a meaningful variance to the verbs crossing and intersecting.



## C.4 Additional Examples

We show examples of models' responses to the prompts on the counting the number of line intersections task in Fig. 5.



**Fig. 32:** All VLMs, except **Sonnet-3.5**, fail at counting when there is no intersection, even when the gap between 2 lines is large (second image on the left).

## D Counting the number of nested squares

### D.1 Benchmark Construction Details

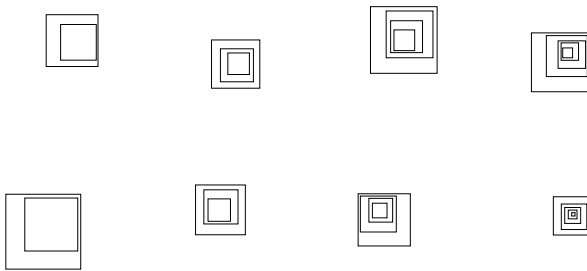
We use 5 parameters to create the images of nested squares.

- **Depth:** For each image, we draw  $N \in \{2, 3, 4, 5\}$  nested squares on the image. We refer to each square in this collection as a depth.
- **Initial size:** We choose a random size for the first square in the bounds of the image size.
- **Reduction factor:** We draw squares such that each depth is entirely contained by its previous depth. We use a reduction factor to scale the square sizes.
- **Center:** The first square’s center is chosen to ensure it is entirely visible in the image. For the remaining squares, we choose the center based on the space between the previous square and the new reduced size.
- **Line thickness:** We use standard *matplotlib* line width parameter of (2, 3, 4).

We continue to generate images until we have 30 samples for each depth, resulting in 120 images overall (see Fig. 33).

**Code** The code is available at <https://anonymous.4open.science/r/Benchmark-85F0/src/NestedSquares/GenerateSamples.ipynb>.

**Post-processing:** We do not ask VLMs to provide answers in a pre-defined format. Instead, we write code to extract predicted labels from VLM free-form response.







(a) 2 squares    (b) 3 squares    (c) 4 squares    (d) 5 squares

**Fig. 33:** Random examples from the nested square task that have 2, 3, 4 or 5 squares in the image.

## D.2 Finding: the best performing models are unaffected by line thickness

Table 10 depicts that the two best VLMs ([Gemini-1.5](#) and [Sonnet-3.5](#)) on the nested square task do not show any sensitivity to the visual attributes of the squares such as the line thickness. However, [GPT-4o](#) and [Sonnet-3](#) have the opposite trend as the line thickness changes, suggesting [GPT-4o](#) confuses squares when the borderline is thick, but, [Sonnet-3](#) can see the squares easier with thicker lines.


**Table 10:** Line thickness has zero to minimal effect on VLMs’ performance, suggesting that visual attributes of shapes are not critical to VLMs when asked to count the shapes.





Category	Metric				
Thickness	2	52.50	80.00	42.50	87.50
	3	45.00	80.00	60.00	87.50
	4	47.50	80.00	62.50	87.50
<b>Average</b>		48.33	80.00	55.00	87.50





## D.3 Additional Examples

We show examples of models’ responses to the counting the number of nested squares task in Fig. 34.

Count total number of squares in the image.



	1	✗	2	✓	5	✗	5	✗	1	✗	6	✗
	2	✓	2	✓	5	✗	5	✗	3	✓	5	✓
	2	✓	4	✗	5	✗	5	✗	4	✗	4	✗
	2	✓	2	✓	4	✓	4	✓	3	✓	4	✗

 [GPT-4o](#)
 [Gemini-1.5](#)
 [Sonnet-3](#)
 [Sonnet-3.5](#)

**Fig. 34:** While all VLMs cannot reliably see and count the squares when the number of shapes increases, [GPT-4o](#) and [Sonnet-3](#) also struggle to count even 2 or 3 squares.

## E Counting the shapes in an Olympic-like logo

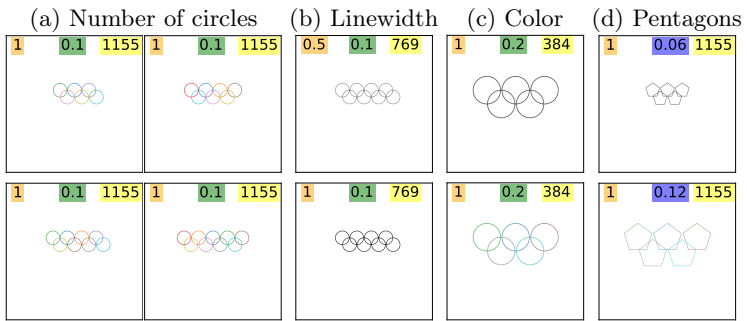
### E.1 Benchmark Construction Details

We create the benchmark by generating images containing shapes resembling the Olympic logo by choosing a combination of settings.

- **Image size:** We fix the physical size of the image in *matplotlib* to  $5 \times 5$ , and change the resolution by changing the DPI value, which is  $\in \{100, 200, 300\}$  to get images with sizes  $\{384, 769, 1155\}$ px.
- **Number of shapes:** We choose a number from  $\{5, 6, 7, 8, 9\}$ .
- **Color:** Each image is generated using two different coloring schemes. We generate an all-black version and a second version by randomly sampling colors from a colormap in *matplotlib*.
- **Distance:** To generate the interlaced shapes, we use a small boundary-to-boundary distance factor for each row of the shapes. We fix this value to 0.1 proportional to the diameter of circles or side length of pentagons.
- **Diameter:** We choose a uniform diameter for all the circles in each image from  $\{\frac{1}{5}, \frac{1}{10}\}$  proportional to the image size.
- **Side length:** We follow the same policy for the diameter to choose the side length of the pentagons.
- **Line thickness:** We generate each image with  $\{0.5, 1.0\}$  line width of *matplotlib* standard numbers.

We center the shape collection on the center of the image in two rows. We ensure for an odd number of shapes, the first row has one more shape, and draw the second row such that the shapes' centers align with the midpoint of the distances in the first row. For even numbers, we repeat the same process as odd numbers. However, we draw an extra shape on the left or right side of the second row randomly. We generate 120 images (see Fig. 35), 60 images of circles, and 60 images of pentagons.

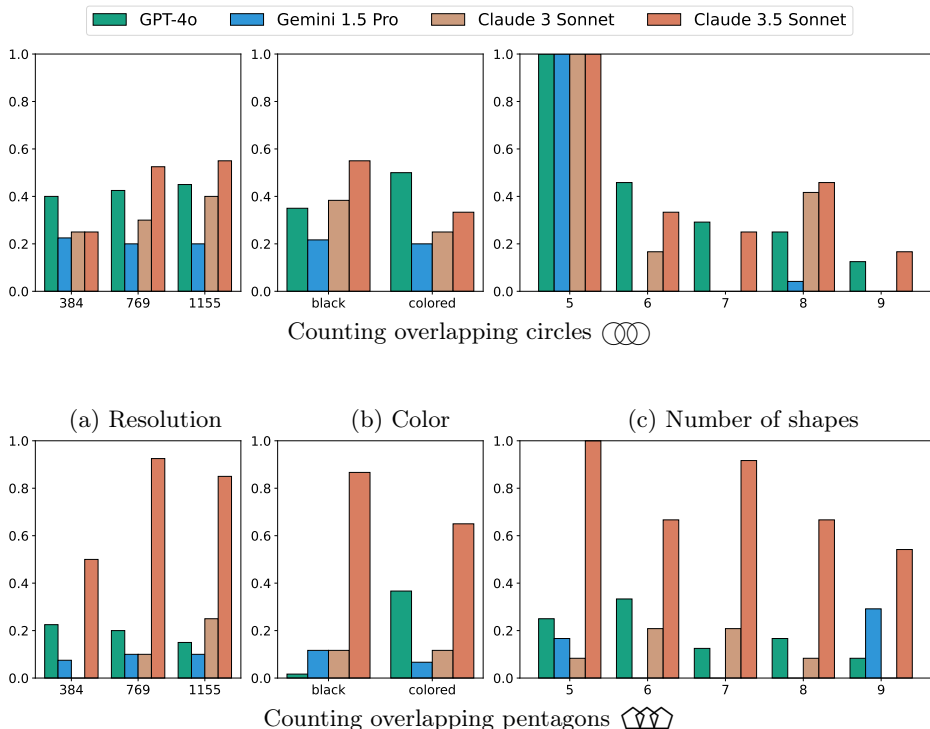
**Code** The code is available at <https://anonymous.4open.science/r/Benchmark-85F0/src/CountingCircles/OlympicCircles.ipynb>.



**Fig. 35:** We generate images of (a) different numbers of circles with various parameter changes, *e.g.*, **the diameter**, (b) **the linewidth** (in points) (c) colorings, and the **image size** (in pixels). For the pentagons, we vary the **side length** instead of the diameter.

## E.2 Finding: different resolutions have no impact on most VLMs' performance

Fig. 36-a shows that VLMs are invariant to the resolution when asked to count the overlapping shapes. This suggests that the image quality has almost no effect on the performance, and VLMs cannot see the shapes.



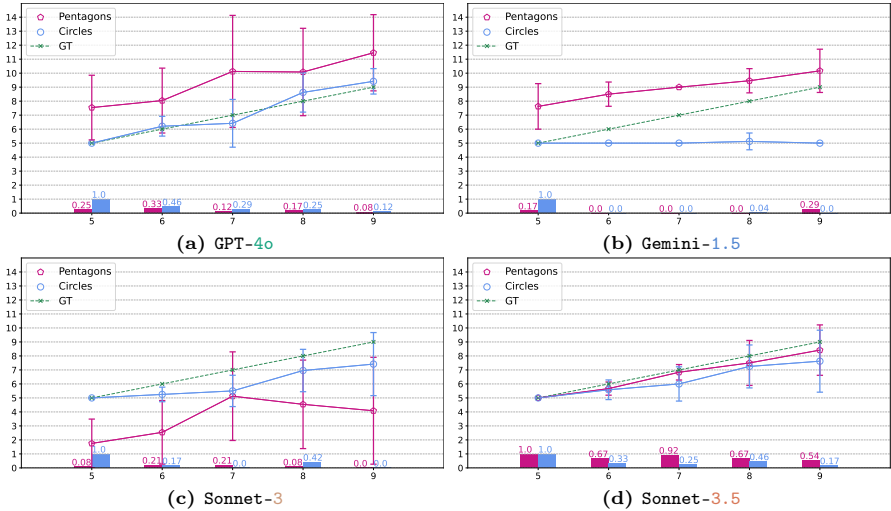
**Fig. 36:** VLMs perform better on counting overlapping circles (○○) (top) than overlapping pentagons (⬠⬠) (bottom). For most models, resolution (a) and colors (b) have minimal impact on performance. **Sonnet-3.5** performs better as the image size increases (a). **GPT-4o** performs better on colored shapes than on black shapes.

## E.3 Finding: color-coding does not generally help the VLMs

While we expect the color-coding to make the shapes more distinct for the models, Fig. 36-b suggests that, except for **GPT-4o**, coloring the shapes has an opposite effect on the performance of the models.

## E.4 Finding: Gemini-1.5 is biased to the Olympic logo

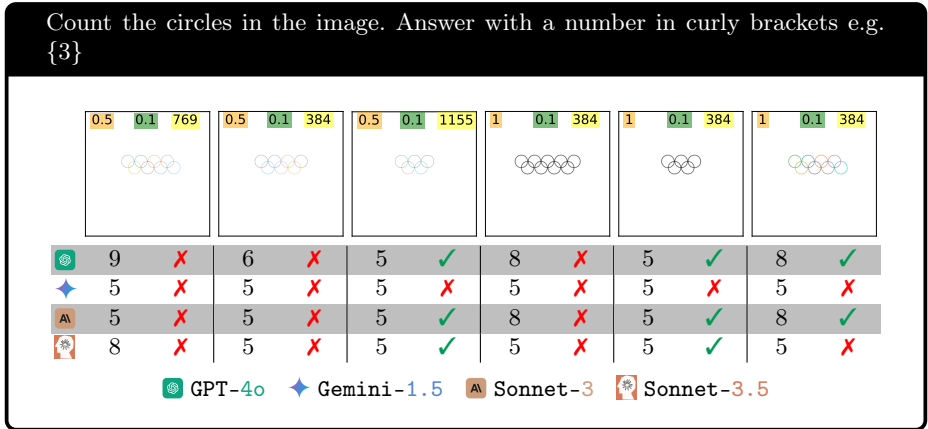
Fig. 37 shows the overall trend of the predictions among SOTA VLMs. **Gemini-1.5** (see Fig. 37b) significantly tends to predict “5” when asked to count the circles, while the predictions are more random for pentagons. This suggests the model’s bias toward the Olympic logo. Among all the models, **Sonnet-3.5** has the least variance (see Fig. 37d).



**Fig. 37:** Prediction trend for each VLM shows (a) **GPT-4o** has less variance in counting circles versus pentagons, (b) **Gemini-1.5** is biased to predict “5” for circles, (c) **Sonnet-3** mostly count fewer shapes than reality, and (d) **Sonnet-3.5** has the least relative variance over both shapes.

## E.5 Additional Examples

We provide examples of VLMs' responses in Figs. 11 and 38



**Fig. 38:** VLMs are correct almost only when the image includes 5 circles supporting the fact that their prediction is biased toward the actual Olympic logo.



## F Counting the rows and columns of a grid task

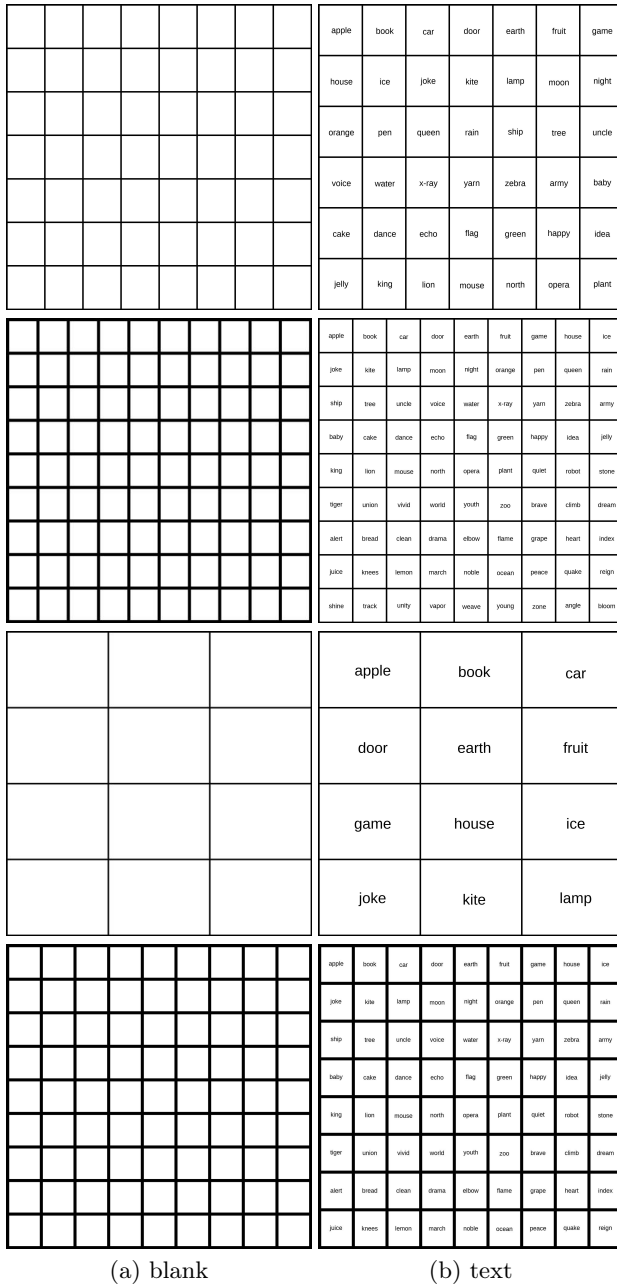
### F.1 Benchmark Construction Details

Our benchmark specifications consist of various parameters for the grid generation process.

- **Image size:** We include three different sizes  $\{500, 1250, 2000\}$  to create the grids on the image.
- **Number of rows/columns:** We choose a base size  $N \in \{3, 4, 5, 6, 7, 8, 9\}$ , and initialize the sizes to  $N \times N$ ,  $N \times N'$ , and  $N' \times N$  where  $N' = N + 1$ .
- **Line thickness:** We use 10 and 20 pixels for the borderline thickness.
- **Entry:** Each table is generated in two versions, one that includes blank entries, and the second with random text entries.

We divide the image size by the number of rows and columns to find the coordinates for drawing the borderlines. Then, we draw the lines on the four edges of the image and draw the remaining lines in between. Our benchmark comprises 444 images of blank and text-containing grids (see Fig. 39).

**Code** The code is available at <https://anonymous.4open.science/r/Benchmark-85F0/src/CountingRowsAndColumns/Grids.ipynb>.







**Fig. 39:** We create grids with various sizes and line thicknesses. Each grid has a blank (a) and text (b) version.

## F.2 Finding: VLMs cannot count the grid cells along different axes

We expect that counting both rows and columns successfully to be harder for the VLMs, thus we analyze counting the rows and grids individually to see how VLMs perform. As shown in Table 11, VLMs cannot count whether rows or columns.

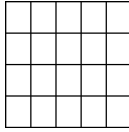
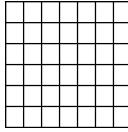
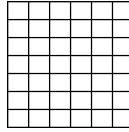
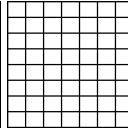
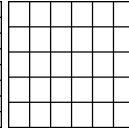
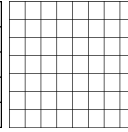







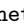
**Table 11:** Average row and column counting accuracy of VLMs show even breaking down the accuracy do not highlight a reliable performance by VLMs in counting uniform-sized cells of a grid.

Axis				
Rows	0.6554	0.4444	0.4219	0.8264
Column	0.5842	0.6597	0.7465	0.9054

## F.3 Additional Examples

We show examples of models' responses to the counting the number of rows and columns task in Figs. 40 and 41.

Count the number of rows and columns and answer with numbers in curly brackets. For example, rows={5} columns={6}

						
GT	4×5	6×7	7×6	8×7	5×6	7×8
	4×4 ❌	6×6 ❌	7×7 ❌	6×6 ❌	6×6 ❌	6×6 ❌
	5×5 ❌	6×6 ❌	7×7 ❌	10×10 ❌	5×6 ✅	10×10 ❌
	5×5 ❌	7×8 ❌	6×6 ❌	9×9 ❌	6×6 ❌	9×12 ❌
	4×5 ✅	6×7 ✅	7×7 ❌	8×7 ✅	5×6 ✅	8×8 ❌
	 GPT-4o	 Gemini-1.5	 Sonnet-3	 Sonnet-3.5		

**Fig. 40:** Examples from the benchmark show that models consistently fail at counting rows and columns of empty grids. **Sonnet-3.5**, however, is more consistent in the lower number of rows and columns.

How many rows and columns are in the table? Answer with only the numbers in a pair (row, column), e.g., (5,6).

GT	4×4	4×5	5×4	5×6	6×7	7×7
	4×4 ✓	4×5 ✓	5×4 ✓	5×6 ✓	6×8 ✗	7×8 ✗
	4×4 ✓	4×5 ✓	5×4 ✓	5×6 ✓	6×8 ✗	7×8 ✗
	4×4 ✓	5×5 ✗	5×4 ✓	6×6 ✗	7×7 ✗	8×7 ✗
	4×4 ✓	4×5 ✓	5×4 ✓	5×6 ✓	6×7 ✓	7×7 ✓

GPT-4o  
 Gemini-1.5  
 Sonnet-3  
 Sonnet-3.5

**Fig. 41:** When text is included in the cells of the grid, the performance of all VLMs improves, especially **Sonnet-3.5**.

## G Following single-colored intersecting paths task

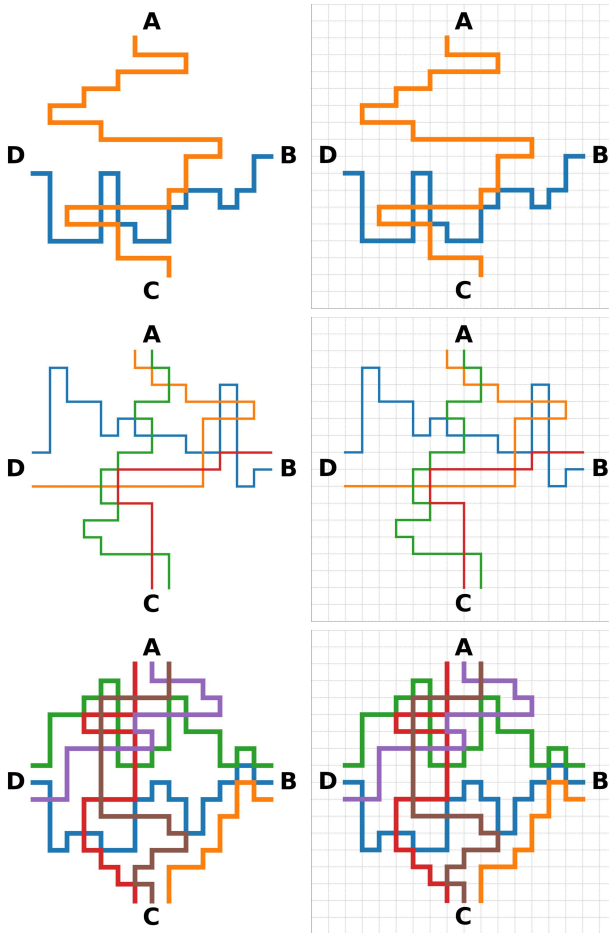
### G.1 Benchmark Construction Details

Our subway-like graphs are generated using a set of parameters defining the characteristics of the plot.

- **Image size:** We use two different sizes {512, 1024}px for the images to include various resolutions.
- **Grid size:** We assume a hypothetical grid on the image that determines the position of the paths. We used an 18×18 grid, which means each path segment is  $\frac{1}{18}$  of the image size.
- **Number of stations:** We use four station labels, {A, B, C, D}.
- **Starting points:** Each station in our maps has three different starting points which are exactly  $\frac{1}{18}$  of the image size to one side of the stations.
- **Path thickness:** We use two line thicknesses, 10 and 20 pixels to have bold and light visualizations of the same path.
- **Number of paths:** Considering the number of starting points in our setup, each image can include stations from which exactly 1, 2, or 3 paths exit.

We keep generating the images until we have 15 samples for each number of paths which results in 180 images (see Fig. 42).

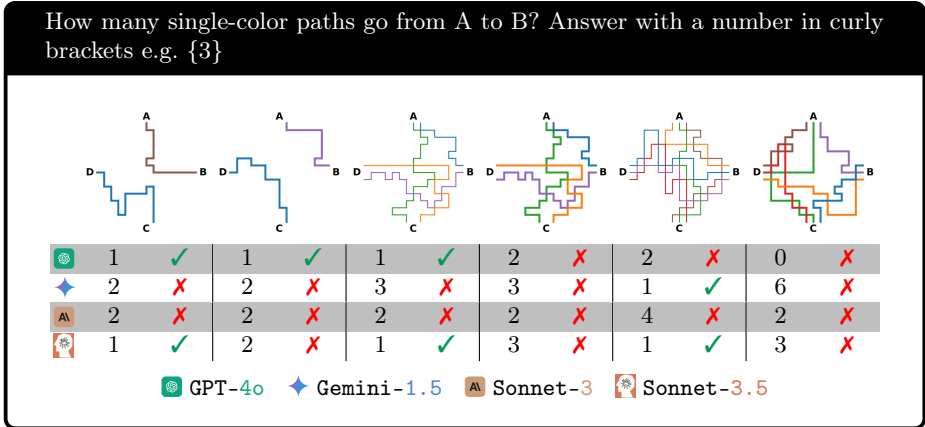
**Code** The code is available at <https://anonymous.4open.science/r/Benchmark-85F0/src/SubwayMap/SubwayMap.ipynb>



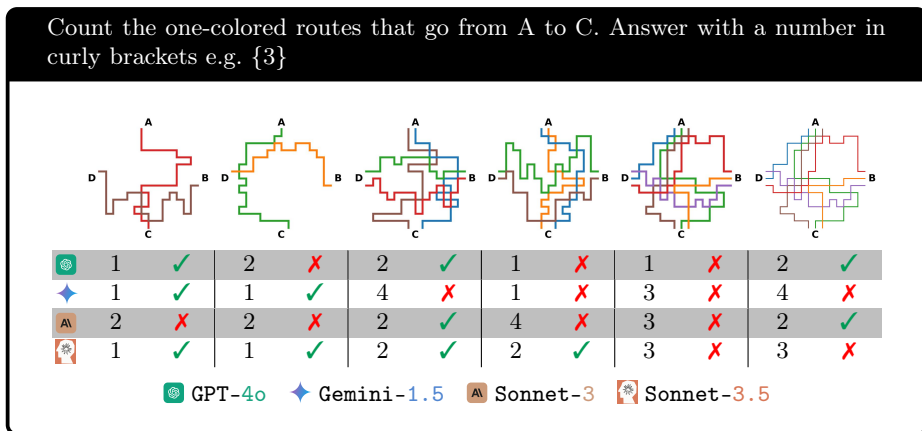
**Fig. 42:** Images in our benchmark (left) have exactly 1, 2, or 3 paths exiting each station. The hypothetical grids (right) are used when generating the paths.

## G.2 Additional Examples

We show examples of models' responses to the counting the number of single-colored connecting paths in Figs. 43 and 44.



**Fig. 43:** VLMs generally fail at images with more intersecting paths. As the number of paths increases, models tend to make an educated guess, especially **Gemini-1.5** and **Sonnet-3.5**.



**Fig. 44:** Gemini-1.5 and Sonnet-3.5 are more consistent at images where 1 path exits each station. GPT-4o and Sonnet-3, however, can easily be fooled on the same image.